[redacted]

Copy 35
RM SL55K07

NACA

RESEARCH MEMORANDUM

for the

U. S. Air Force

INVESTIGATION OF A 1/4-SCALE MODEL OF THE REPUBLIC F-105 AIRPLANE IN THE LANGLEY 19-FOOT PRESSURE TUNNEL

LONGITUDINAL STABILITY AND CONTROL AND HORIZONTAL-TAIL HINGE-MOMENT AND NORMAL-FORCE CHARACTERISTICS OF THE MODEL EQUIPPED WITH A DROOPED SUPERSONIC-TYPE ELLIPTICAL WING-ROOT INLET

By Patrick A. Cancro and H. Neale Kelly

Langley Aeronautical Laboratory
Langley Field, Va.

[redacted]

NATIONAL ADVISORY COMMITTEE
FOR AERONAUTICS
WASHINGTON

[redacted]

NACA RM SL55K07

NATIONAL ADVISORY COMMITTEE FOR AERONAUTICS

RESEARCH MEMORANDUM

for the

U. S. Air Force

INVESTIGATION OF A 1/4-SCALE MODEL OF THE REPUBLIC F-105 AIRPLANE IN THE LANGLEY 19-FOOT PRESSURE TUNNEL

LONGITUDINAL STABILITY AND CONTROL AND HORIZONTAL-TAIL HINGE-MOMENT AND NORMAL-FORCE CHARACTERISTICS OF THE MODEL EQUIPPED WITH A DROOPED SUPERSONIC-TYPE ELLIPTICAL WING-ROOT INLET

By Patrick A. Cancro and H. Neale Kelly

SUMMARY

Low-speed development tests on a 1/4-scale model of the Republic F-105 airplane have been conducted in the Langley 19-foot pressure tunnel. The present paper contains the results of additional longitudinal stability tests and of measurements of the hinge moments and normal force of the all-movable horizontal tail on the model equipped with a supersonic-type elliptical wing-root inlet.

These tests were made at a Reynolds number of 9.0×10^6 and a Mach number of 0.20. The longitudinal stability characteristics of the model equipped with an all-movable horizontal tail, with and without speed brakes, and with and without various external stores, were determined with the leading- and trailing-edge flaps retracted and extended.

The horizontal-tail hinge-moment and normal-force measurements were made at various horizontal stabilizer settings with the leading-edge flaps retracted and extended.

In order to expedite the issuance of data for this airplane, no analysis of the data has been presented.

INTRODUCTION

The F-105 airplane is a 45° sweptback, midwing, low-tail, supersonic fighter bomber being developed by the Republic Aviation Corporation for the U. S. Air Force. At the request of the Air Force, development tests on a 1/4-scale model of the F-105 airplane have been conducted in the Langley 19-foot pressure tunnel to determine the low-speed aerodynamic characteristics of the basic design and, if necessary, to develop modifications which will provide the model with satisfactory low-speed stability and control characteristics.

References 1, 2, and 3 contain the results of low-speed longitudinal stability and control tests on a 1/4-scale model of the F-105 airplane and some exploratory lateral control tests. (ref. 1 only). The results of supersonic and high subsonic tests on a 1/22-scale model of the F-105 airplane are contained in references 4 and 5.

Presented herein are the results of additional longitudinal stability tests and tail hinge-moment and normal-force tests of the model equipped with a drooped supersonic-type elliptical wing-root inlet.

The basic model for the present tests is the same as that of reference 3.

COEFFICIENTS AND SYMBOLS

C_L lift coefficient, $\frac{\text{Lift}}{qS_W}$

C_m pitching-moment coefficient, $\frac{\text{Pitching moment}}{qS_W\bar{c}}$ (an additional subscript denotes location of center of gravity)

C_D drag coefficient, $\frac{\text{Drag}}{qS_W}$

C_{N_t} tail normal-force coefficient, $\frac{\text{Tail normal force}}{qS_{te}}$

C_{h_t} tail hinge-moment coefficient about $0.098\bar{c}$ of the horizontal tail, $\frac{\text{Tail hinge moment}}{q(S\bar{c})_{te}}$

[redacted]

b	wing span, ft
$\bar{c}$	mean aerodynamic chord, $\frac{2}{S}\int_0^{b/2} c^2 dy$, ft
c	local streamwise chord, ft
q	free-stream dynamic pressure, lb/sq ft
S	area, sq ft
y	spanwise distance from plane of symmetry, ft
α	angle of attack, deg
i_t	tail incidence relative to the wing-chord plane, trailing edge down for positive incidence, deg

Subscripts:

te	horizontal tail not covered by the fuselage
W	wing

MODEL

Model Description

The model was primarily of steel-reinforced wood construction; however, the inlets, trailing-edge flaps and leading-edge flaps were aluminum. Principal dimensions and design characteristics of the model may be found in table I.

Basic model.- The basic model for these tests was a 1/4-scale model of the F-105 airplane wing, fuselage, and vertical tail. A three-view drawing of the model and a photograph showing the model mounted in the tunnel are presented in figures 1 and 2.

Horizontal tail.- The horizontal tail was located at a tail height of $0.123b/2$ below the mean-aerodynamic-chord plane extended. Tail incidences of -14°, $\pm 7^\circ$, $\pm 3.5^\circ$, and 0° were investigated. A resistance-type electrical strain-gage balance was employed to measure the tail hinge moments and normal forces. (See fig. 3.)

Inlet.- The model was equipped with a drooped supersonic-type elliptical wing-root inlet. This inlet was similar to the supersonic inlet of

[redacted]

references 1 and 2 except that the area ahead of the droop line (see fig. 4) was drooped approximately 5° and the inlet side body was faired into the contour of the wing with the leading-edge flap deflected 7.5°.

Trailing-edge flaps.- The wing was equipped with a single-slotted trailing-edge flap which extended from 0.133b/2 to 0.700b/2. Flap deflections of 0° and 46° perpendicular to the flap hinge line were obtained through the use of interchangeable steel positioning brackets. Dimensions of the flap and flap gap are presented in figure 5.

Leading-edge flaps.- An inversely tapered drooped leading-edge flap with interchangeable deflection brackets of 0°, 7.5°, and 20° measured perpendicular to the hinge line was provided as a stall-control device. Details of the leading-edge flaps are shown in figure 5.

External stores.- External stores of two types representative of 450-gallon pylon-mounted fuel tanks were tested. Attachment point for both the type I (fineness ratio 10.25) and the type II (fineness ratio 7.81) tanks was at the 0.606b/2 wing station. Figure 6 contains a sketch and pertinent details of the store configurations.

Speed brakes.- Speed-brake panels were provided that could be attached to the rear end of the fuselage (see fig. 6) at a deflection of 50° in both the vertical and the horizontal planes.

Model Nomenclature

Listed below are the designations given to the various component parts of the model. The complete model configurations are obtained by combining the appropriate model components with the basic model.

A — basic model (wing plus fuselage)

B — speed brakes
- first subscript: vertical deflection, deg
- second subscript: horizontal deflection, deg

E — external stores
- subscript: 0 indicates outboard location (0.606b/2)
- suffix: 450 (type I) indicates 450-gallon store of fineness ratio 10.25
  450 (type II) indicates 450-gallon store of fineness ratio 7.81

F — single slotted trailing-edge flap
- prefix: flap span (fraction of wing semispan)
- subscript: deflection, trailing edge down for positive deflection, deg

I wing-root inlet
subscript: SE' indicates drooped supersonic-type elliptical inlet

N inversely tapered drooped leading-edge flap
subscript: deflection, leading edge down for positive deflection, deg

T horizontal tail
prefix: vertical position (fraction of wing semispan)
subscript: incidence, trailing edge down for positive deflection, deg

V vertical tail

TESTS

All tests reported herein were conducted in the Langley 19-foot pressure tunnel at a tunnel pressure of approximately $2\frac{1}{3}$ atmospheres. A Reynolds number of 9.0×10^6 and a Mach number of 0.20 were maintained throughout the tests.

The model was mounted on the normal three-support system (see fig. 2) at 0° angle of yaw and was tested through an angle-of-attack range of -4° to 29°. Longitudinal stability characteristics of the model with the horizontal tail set at various incidences with and without speed brakes and stores were determined with the leading-edge and trailing-edge flaps retracted and extended.

The horizontal-tail hinge-moment and normal-force coefficients were determined for various tail incidences with the leading-edge flap retracted and extended.

CORRECTIONS

Jet-boundary corrections determined by the method of reference 6 have been applied to all force and pitching-moment data. Corrections for support tare and interference effects and for air-flow misalinement have not been applied. Internal drag of the inlets and duct system is included in the drag data presented herein.

[redacted]

PRESENTATION OF DATA

The results of the longitudinal stability characteristics of the 1/4-scale model of the Republic F-105 airplane may be found in figures 7 to 15. Horizontal-tail hinge-moment coefficients and normal-force coefficients obtained in this investigation may be found in figures 16 and 17.

Langley Aeronautical Laboratory,
National Advisory Committee for Aeronautics,
Langley Field, Va., November 14, 1955.

H. Neale Kelly
Aeronautical Research Scientist

Patrick A. Cancro
Mechanical Engineer

Approved: Eugene C. Draley
Eugene C. Draley
Chief of Full-Scale Research Division

mfd

[redacted]

REFERENCES

1. Kelly, H. Neale, and Cancro, Patrick A.: Investigation of a 1/4-Scale Model of the Republic F-105 Airplane in the Langley 19-Foot Pressure Tunnel - Longitudinal Stability and Control of the Model Equipped With a Supersonic-Type Elliptical Wing-Root Inlet. NACA RM SL54F28, U. S. Air Force, 1954.

2. Cancro, Patrick A., and Kelly, H. Neale.: Investigation of a 1/4-Scale Model of the Republic F-105 Airplane in the Langley 19-Foot Pressure Tunnel - Influence of Trailing-Edge Flap Span and Deflection on the Longitudinal Characteristics. NACA RM SL54H27, U. S. Air Force, 1954.

3. Cancro, Patrick A., and Kelly, H. Neale: Investigation of a 1/4-Scale Model of the Republic F-105 Airplane in the Langley 19-Foot Pressure Tunnel - Lateral Control and Directional Stability and Control Characteristics of the Model Equipped With a Drooped, Supersonic-Type Elliptical Wing-Root Inlet. NACA RM SL55J10, U. S. Air Force, 1955.

4. Spearman, M. Leroy, Driver, Cornelius, and Robinson, Ross B.: Aerodynamic Characteristics of Various Configurations of a Model of a 45° Swept-Wing Airplane at a Mach Number of 2.01. NACA RM L54J08, 1955.

5. Sleeman, William C., Jr., and Hayes, William C., Jr.: Experimental Investigation at High Subsonic Speeds of the Rolling-Stability Derivatives of a 1/22-Scale Model of the Republic F-105 Airplane. NACA RM SL55F16, U. S. Air Force, 1955.

6. Sivells, James C., and Salmi, Rachel M.: Jet-Boundary Corrections for Complete and Semispan Swept Wings in Closed Circular Wind Tunnels. NACA TN 2454, 1951.

[redacted]

TABLE I

DESIGN CHARACTERISTICS OF THE REPUBLIC F-105 AIRPLANE AND THE 1/4-SCALE MODEL OF THE F-105 AIRPLANE

	Full-scale	1/4-scale
Wing assembly		
Basic data:		
Root airfoil, measured parallel to airplane center line at 0.38b/2	NACA 65A005.5	NACA 65A005.5
Tip airfoil, measured parallel to airplane center line	NACA 65A003.7	NACA 65A003.7
Angle of incidence, deg	0	0
Geometric twist, deg	0	0
Sweep of quarter-chord line (true), deg	45	45
Taper ratio	0.467	0.467
Aspect ratio (excluding inlet area)	3.182	3.182
Dihedral, deg	-3.5	-3.5
Dimensions:		
Root chord (theoretical), parallel to airplane center line, ft	15.000	3.750
Tip chord (theoretical), parallel to airplane center line, ft	7.000	1.750
Mean aerodynamic chord, parallel to airplane center line, ft	11.485	2.871
Location of mean aerodynamic chord, spanwise (projected), ft	7.690	1.933
Span, measured normal to airplane center line, ft	34.934	8.734
Area:		
Wing area (excluding inlet area), sq ft	385.0	24.062
Horizontal-tail assembly		
Basic data:		
Root airfoil, streamwise	NACA 65A006	NACA 65A006
Tip airfoil, streamwise	NACA 65A004	NACA 65A004
Angle of incidence, deg	+7 to -25	+7 to -25
Dihedral, deg	0	0
Taper ratio	0.456	0.456
Aspect ratio	3.06	3.06
Dimensions:		
Root chord (theoretical), ft	7.50	1.875
Tip chord (theoretical), ft	3.42	0.855
Mean aerodynamic chord (theoretical), ft	5.71	1.428
Mean aerodynamic chord (exposed), ft	5.08	1.270
Span, ft	16.67	4.168
0.25$\bar{c}$ of wing to 0.25$\bar{c}$ of horizontal tail (theoretical), ft	20.68	5.232
Vertical location below fuselage center line, in.	-18.00	-4.50
Area:		
Horizontal-tail area (theoretical), sq ft	90.97	5.685
Horizontal-tail area (exposed), sq ft	60.77	3.798

[redacted]

TABLE I.- Continued

DESIGN CHARACTERISTICS OF THE REPUBLIC F-105 AIRPLANE AND THE 1/4-SCALE MODEL OF THE F-105 AIRPLANE

	Full-scale	1/4-scale
Vertical-tail assembly		
Basic data:		
Root airfoil, measured parallel to airplane center line at 0.167b/2	NACA 65A006	NACA 65A006
Tip airfoil, measured parallel to airplane center line	NACA 65A004	NACA 65A004
Sweepback of quarter-chord line, deg	45	45
Aspect ratio (theoretical)	1.593	1.593
Taper ratio (theoretical)	0.365	0.365
Sweepback of rudder hinge line, deg	29.358	29.358
Dimensions:		
Root chord (theoretical), ft	10.03	2.508
Tip chord (theoretical), ft	3.67	0.9175
Mean aerodynamic chord (theoretical), ft	7.34	1.835
$0.25\bar{c}$ of wing to $0.25\bar{c}$ of vertical tail (theoretical), ft	17.40	4.412
Vertical-tail height, measured from fuselage center line, ft	10.92	2.729
Rudder chord (average), ft	1.86	0.458
Rudder span, measured normal to fuselage center line, ft	6.83	1.708
Area:		
Vertical-tail area (theoretical), sq ft	74.8	4.670
Vertical-tail area (exposed), sq ft	48.0	3.000
Rudder area (including overhang), sq ft	11.39	0.712
Fuselage		
Length, ft	62.0	15.049
Maximum width, ft	4.375	1.094
Maximum height (excluding canopy), ft	6.50	1.625
Volume (including canopy), cu ft	1142	17.87
Location of station 0 (measured upstream from nose of airplane), in.	39.672	9.918
Side area (excluding vertical tail), sq ft	346	21.6
Frontal area (including canopy), sq ft	24.7	1.542
Trailing-edge flaps		
Basic data:		
Type	Single slotted	Single slotted
Deflection, measured in a plane normal to 0.82c, deg	0 to 46.2	0 and 46
Dimensions:		
Average chord, measured parallel to airplane center line	0.25c	0.25c
Span (one flap), measured normal to airplane center line, ft	11.7	2.925
Location of outboard edge, measured normal to airplane center line, in.	168.0	42
Location of inboard edge, measured normal to airplane center line, in.	27.85	6.963
Area:		
Area of both trailing-edge flaps, sq ft	67.6	4.23

[redacted]

TABLE I.- Concluded

DESIGN CHARACTERISTICS OF THE REPUBLIC F-105 AIRPLANE AND THE 1/4-SCALE MODEL OF THE F-105 AIRPLANE

	Full-scale	1/4-scale
Leading-edge flaps		
Basic data:		
Type	Drooped nose	Drooped nose
Deflection, measured in a plane normal to hinge line, deg	0 to 20	0,7.5,20
Location of inboard edge, measured normal to airplane center line, in.	82.149	20.537
Location of outboard edge, measured normal to airplane center line, in.	199.78	49.945
Dimensions:		
Average leading-edge flap chord (streamwise)	0.12c	0.12c
Span (one flap), measured normal to airplane center line, ft	9.8	2.45
Area:		
Area of both leading-edge flaps, sq ft	22.7	1.419
External tanks (450-gallon capacity for wing pylon)		
Type I		
Fineness ratio	----------	9.76
Length in.	----------	70.500
Diameter (max.), in.	----------	6.88
Angle of incidence, relative to fuselage center line, deg	----------	3
Spanwise location, measured normal to fuselage, center line, in.	----------	31.75
Vertical location of tank nose, measured below fuselage center line, in.	----------	-10.395
Longitudinal location of tank nose, measured from fuselage station 0, in.	----------	86.558
Type II		
Fineness ratio	7.81	7.81
Length, in.	227.55	56.89
Diameter (max.), in.	29.0	7.25
Angle of incidence, relative to fuselage center line, deg	3	3
Spanwise location, measured normal to fuselage center line, in.	129.0	31.75
Vertical location of tank nose, measured from fuselage center line, in.	-40.04	-10.01
Longitudinal location of tank nose, measured from fuselage station 0, in.	391.16	97.79
Tank fin		
Area of two fins (theoretical projected), sq ft	6.0	1.5
Sweep, deg	40	40
Aspect ratio	2.67	2.67
Taper ratio	1.0	1.0
Span, ft	4.0	1.0
Dihedral, deg	15	15
Speed Brakes		
Location, measured from fuselage station 0		
Top and bottom, in.	728.0	181.75
Sides, in.	739.5	184.75
Area:		
Top and bottom, sq ft	17.5	1.090
Sides, sq ft	11.0	0.690
Deflection:		
Top and bottom, measured normal to hinge line, deg	0 to 45	50
Sides, measured normal to hinge line, deg	0 to 40	50

[redacted]

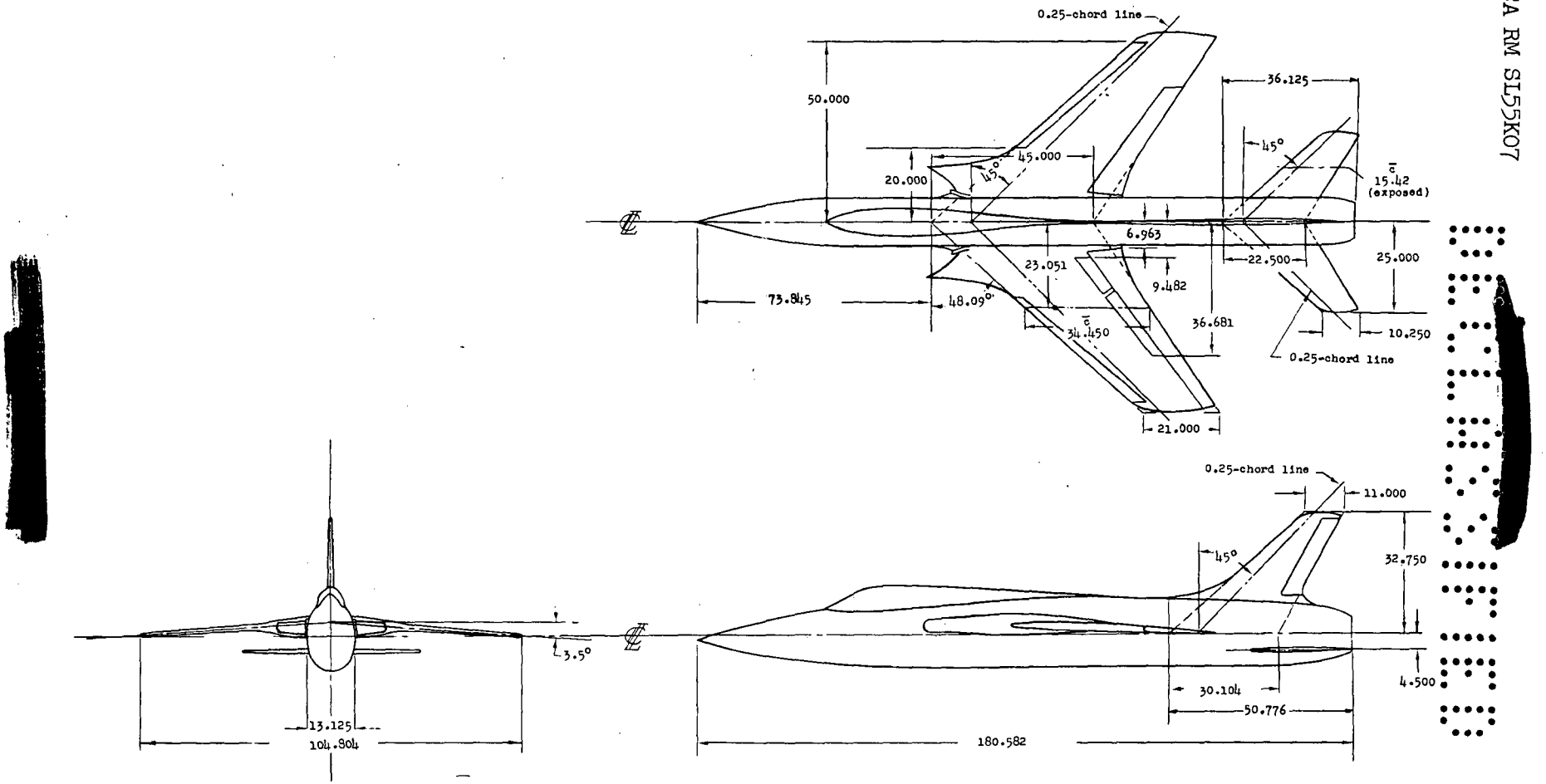

Figure 1.- Three-view drawing of a 1/4-scale model of the Republic F-105 airplane. (Dimensions in inches unless otherwise noted.)

L-84117

Figure 2.- The 1/4-scale model of the Republic F-105 airplane mounted in the Langley 19-foot pressure tunnel.

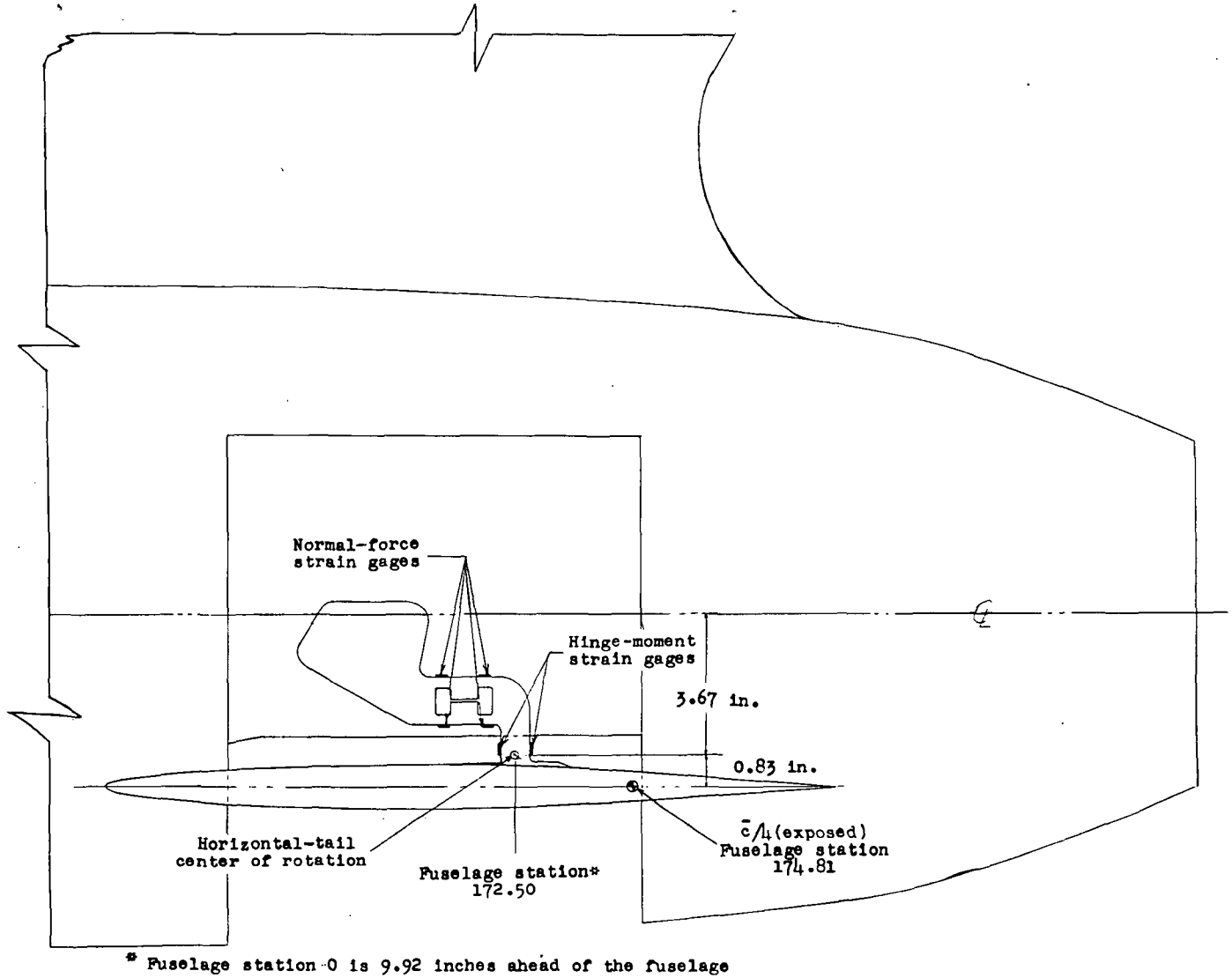

* Fuselage station 0 is 9.92 inches ahead of the fuselage

Figure 3.- Location of the horizontal-tail strain-gage balance.

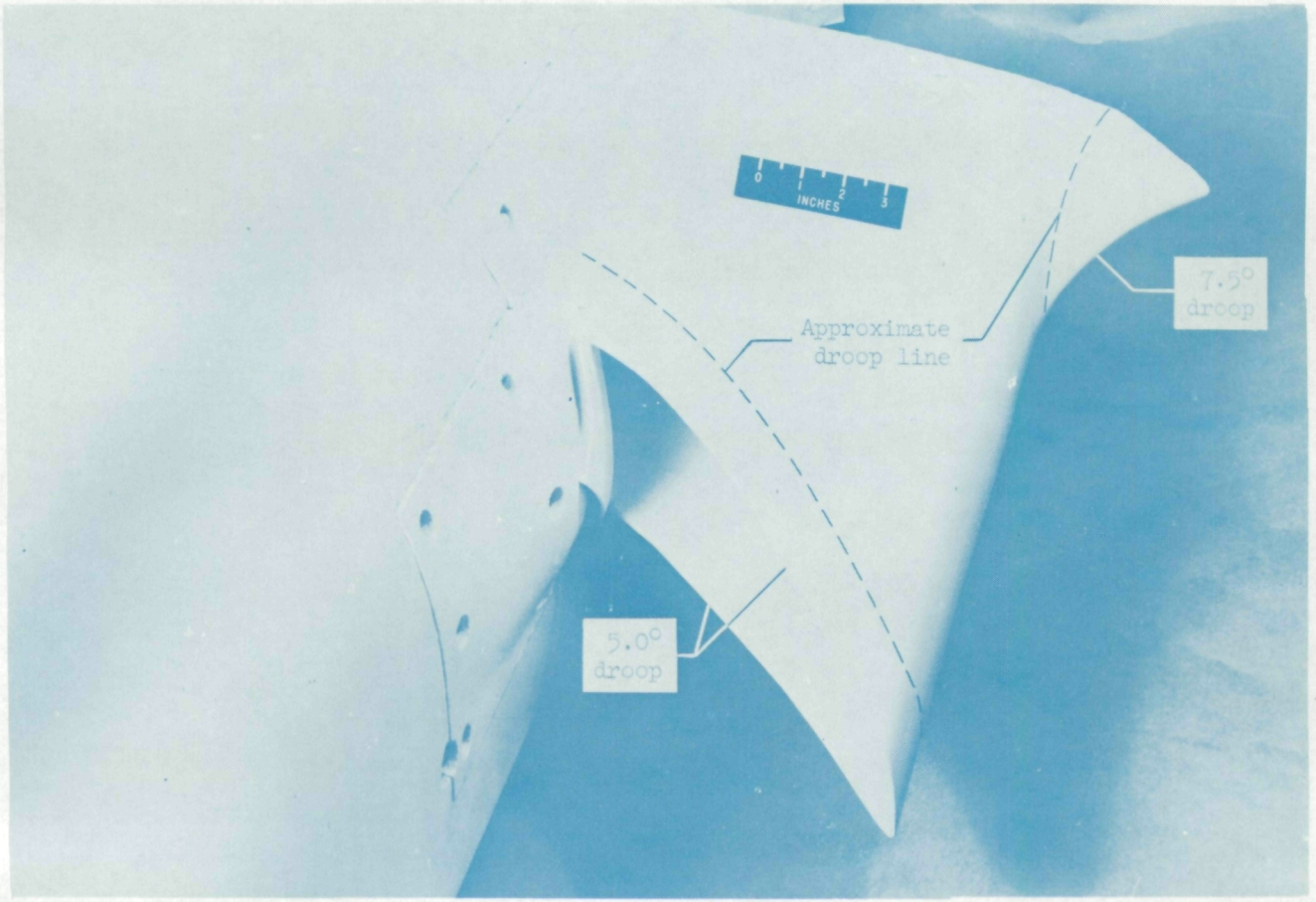

Figure 4.- Supersonic-type elliptical wing-root inlet showing the approximate lines of droop.

L-85123.1

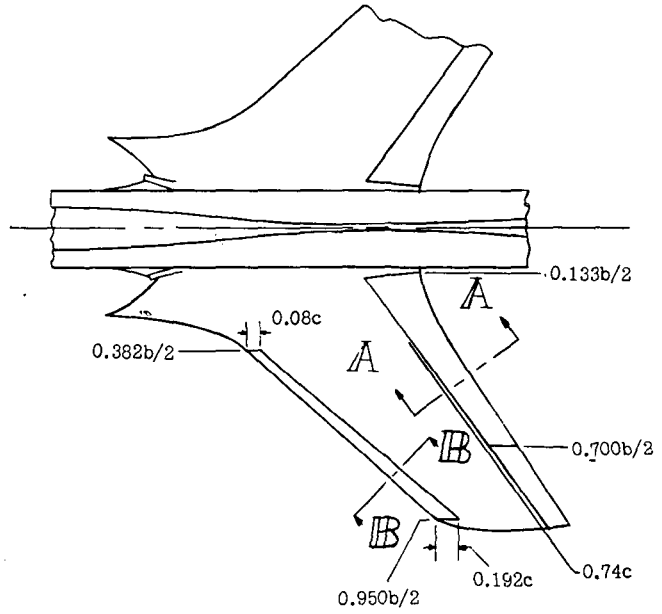

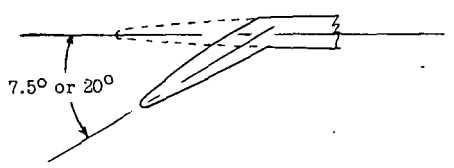

Section B-B
(enlarged)
Typical

(a) Leading-edge flap.

Wing Flap Data
(46° deflection only)

Flap station b/2	Deflection			Flap gap, inches			Fore and aft position, inches		
	Actual		Loft	Actual		Loft	Actual		Loft
	L.H.	R.H.		L.H.	R.H.		L.H.	R.H.	
0.242	46°49'	46°26'	46°13'	0.41	0.40	0.415	2.72	2.73	2.72
.415	46°42'	46°45'	46°13'	.31	.32	.350	2.92	2.91	2.90
.647	46°34'	46°54'	46°13'	--	--	--	--	--	--
.669	--	--	--	.345	.34	.295	2.45	2.47	2.47

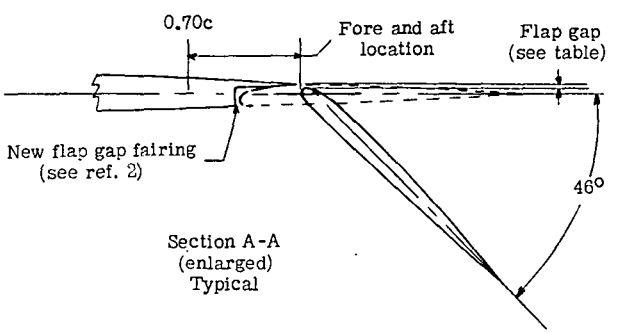

Section A-A
(enlarged)
Typical

(b) Trailing-edge flap.

Figure 5.- Details of the leading- and trailing-edge flaps.

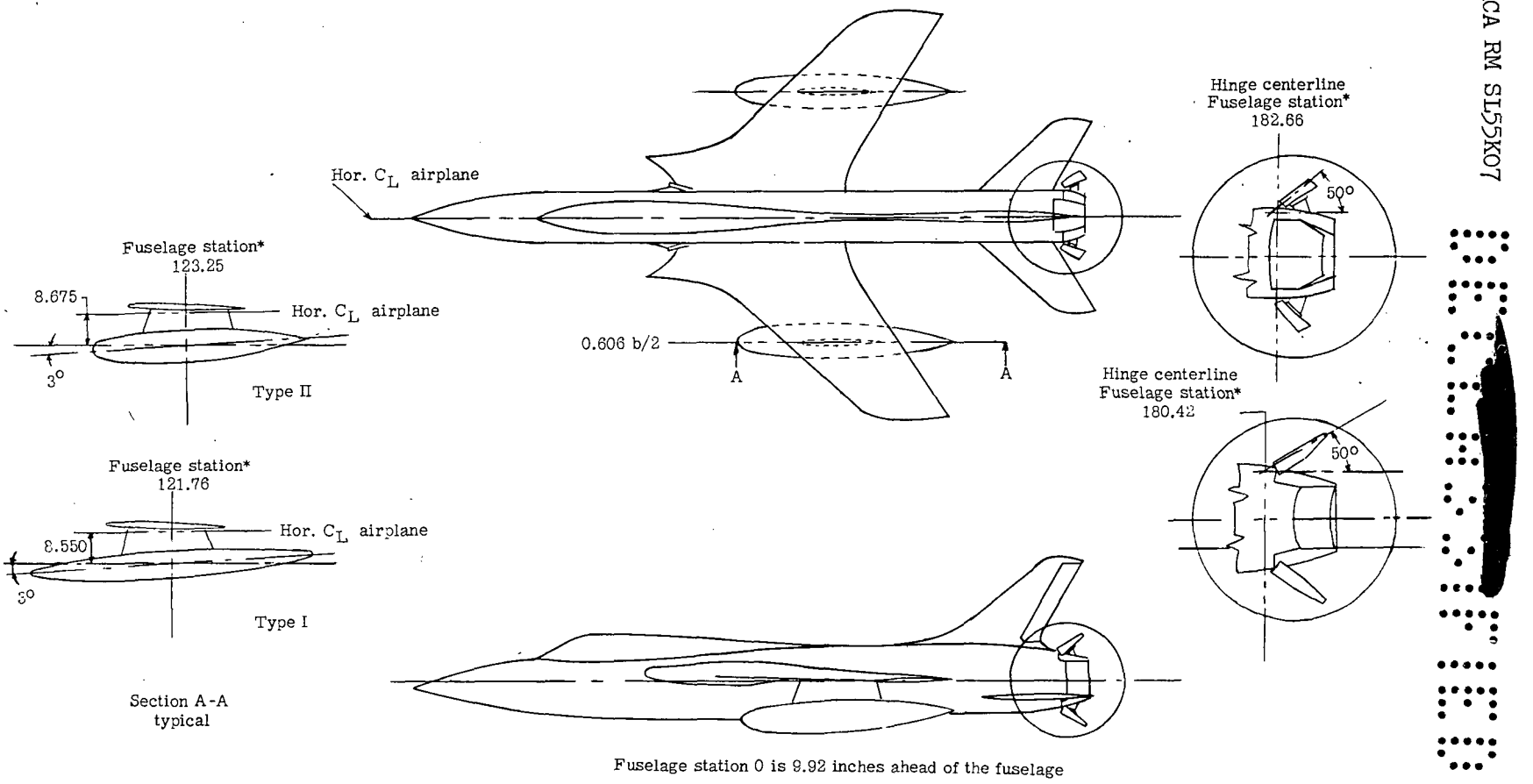

(a) External stores.

(b) Speed brakes.

Figure 6.- Details of the external stores and dive brakes of the 1/4-scale model of the Republic F-105 airplane. (All dimensions in inches except where noted.)

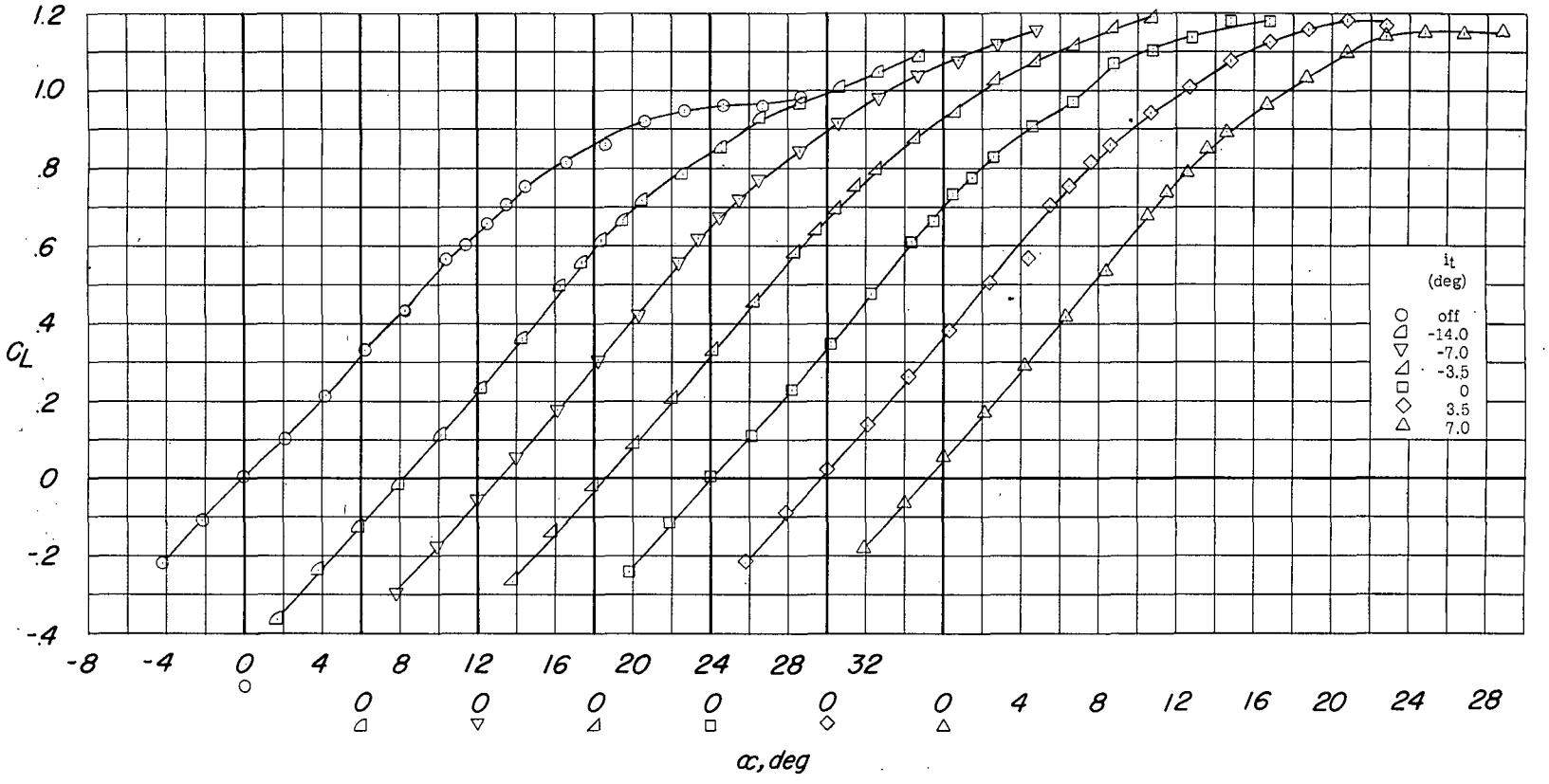

(a) C_L against α.

Figure 7.- Longitudinal stability and control characteristics of the model. Configuration A + V + $I_{SE'}$ + (-0.123)T.

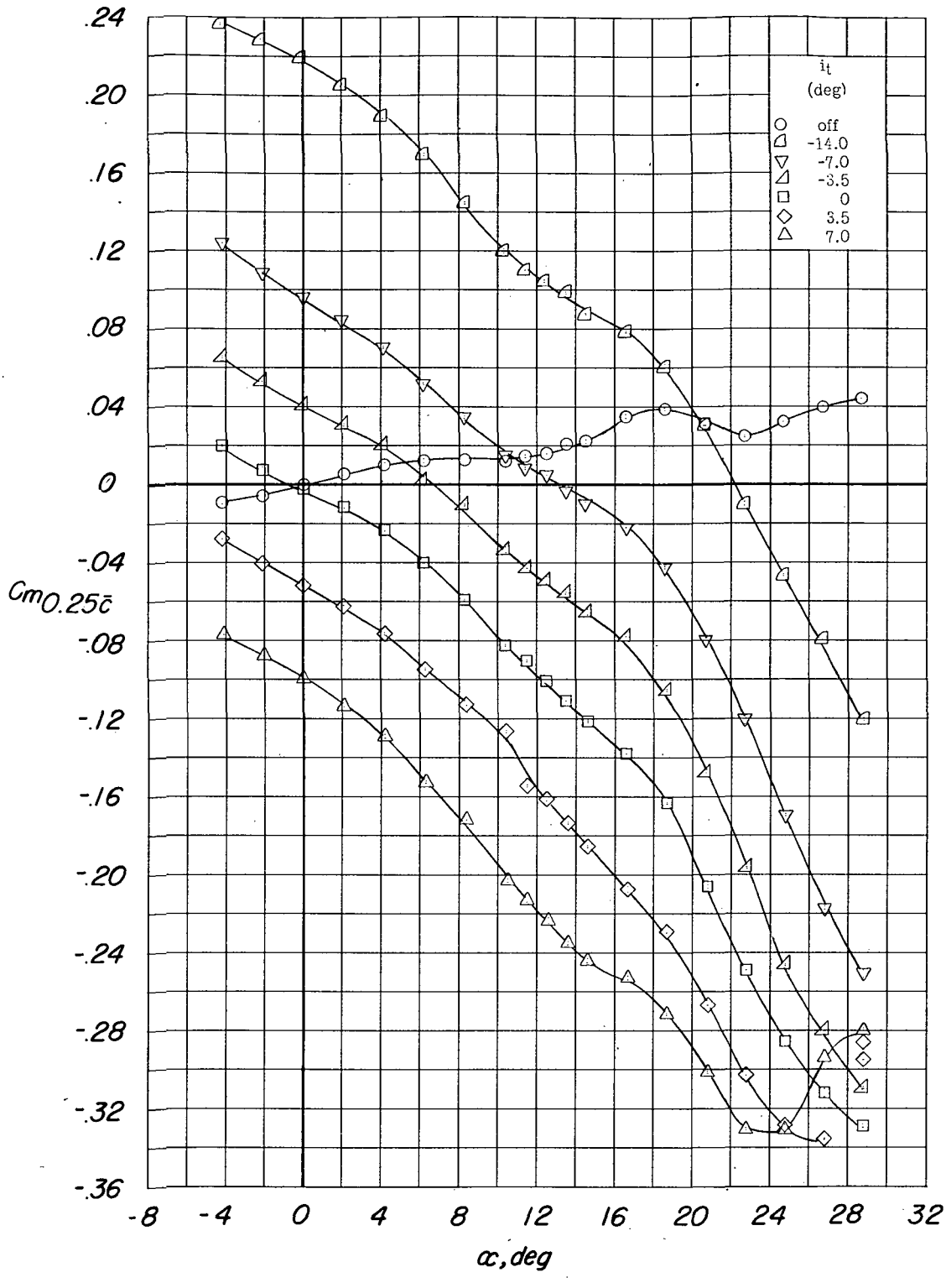

(b) $C_{m_{0.25\bar{c}}}$ against α.

Figure 7.- Continued.

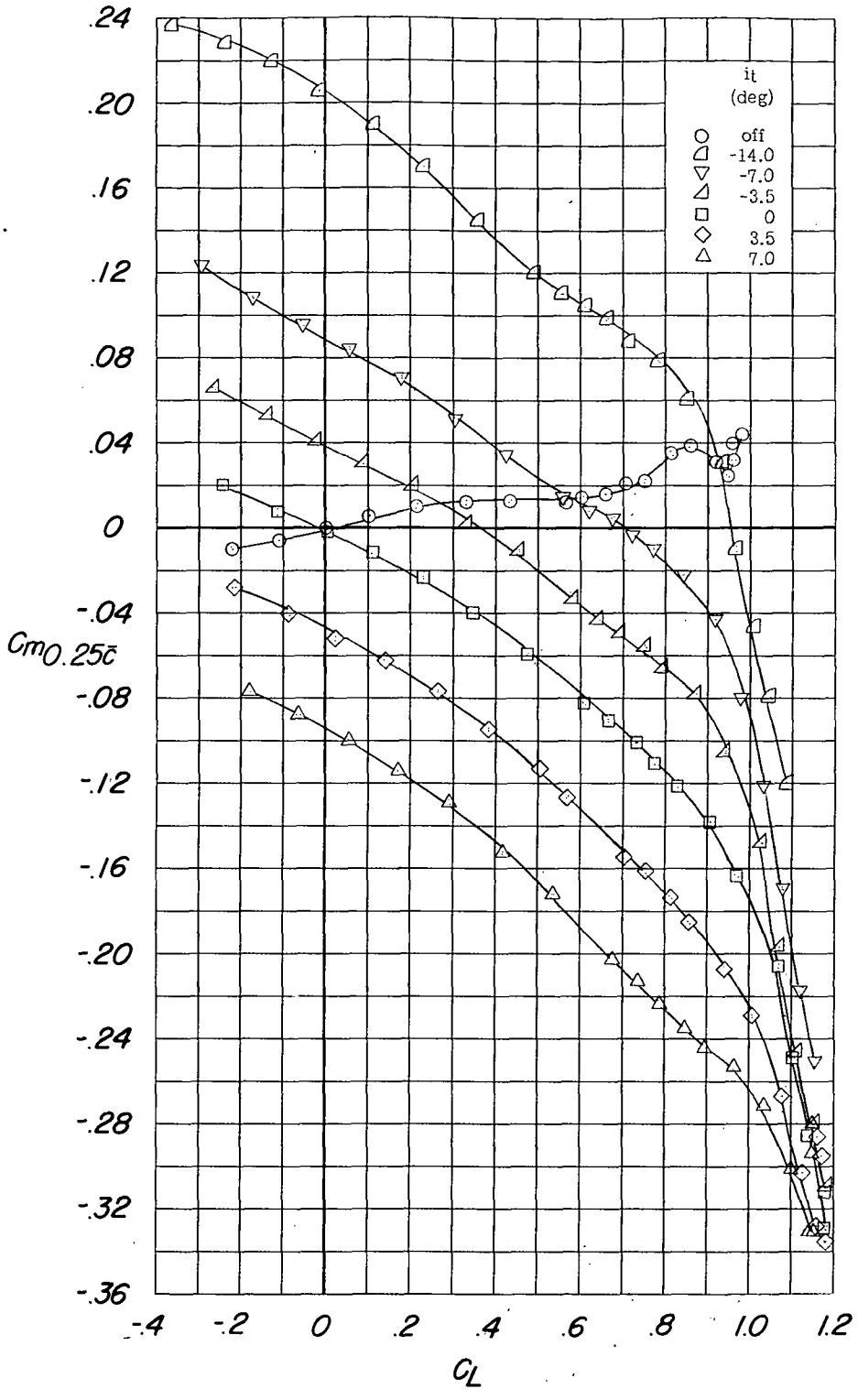

(c) $C_{m_{0.25\bar{c}}}$ against C_L.

Figure 7.- Continued.

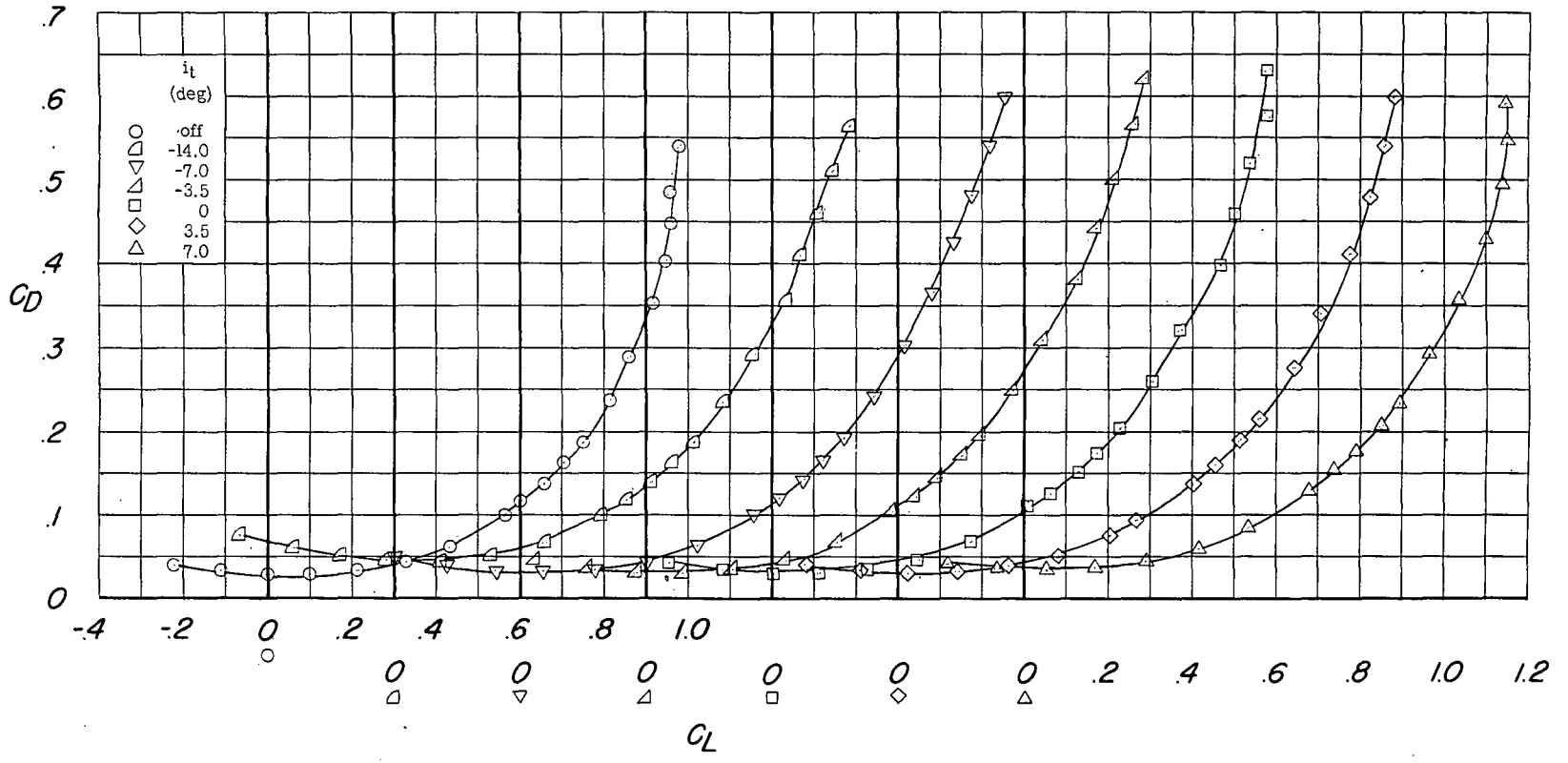

(d) C_D against C_L.

Figure 7.- Concluded.

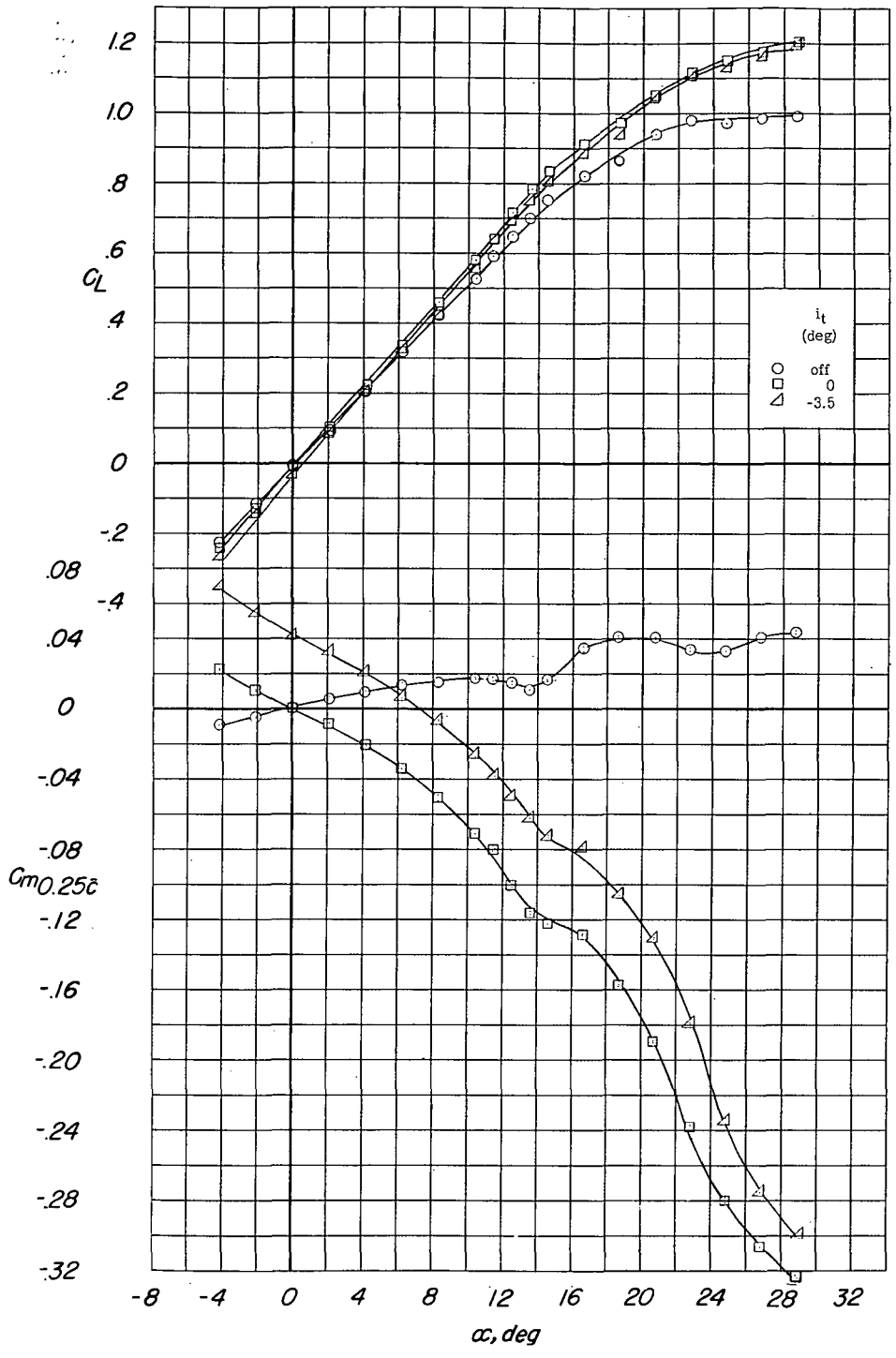

(a) C_L and $C_{m_{0.25\bar{c}}}$ against α.

Figure 8.- Longitudinal stability characteristics of the model with the leading-edge flap deflected. Configuration A + V + $I_{SE'}$ + $N_{7.5}$ + (-0.123)T.

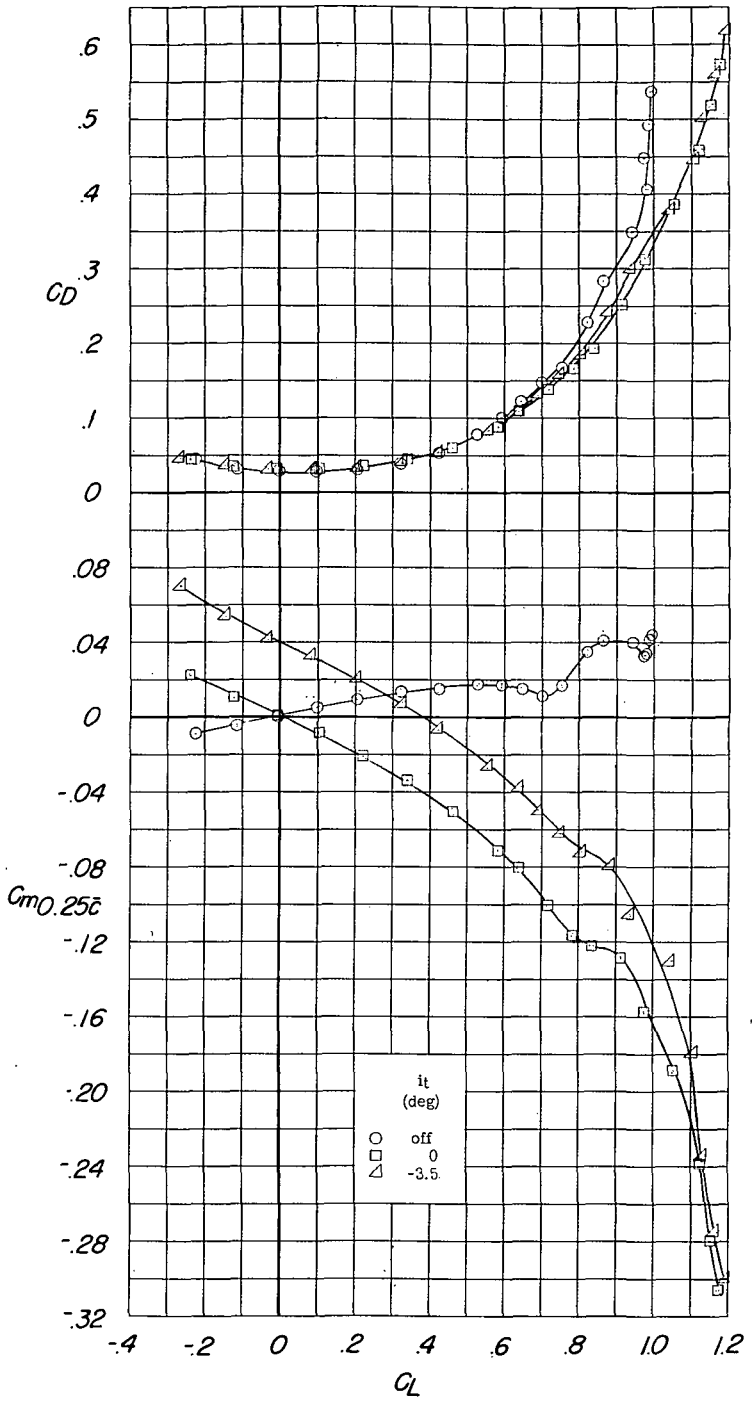

(b) C_D and $C_{m_{0.25\bar{c}}}$ against C_L.

Figure 8.- Concluded.

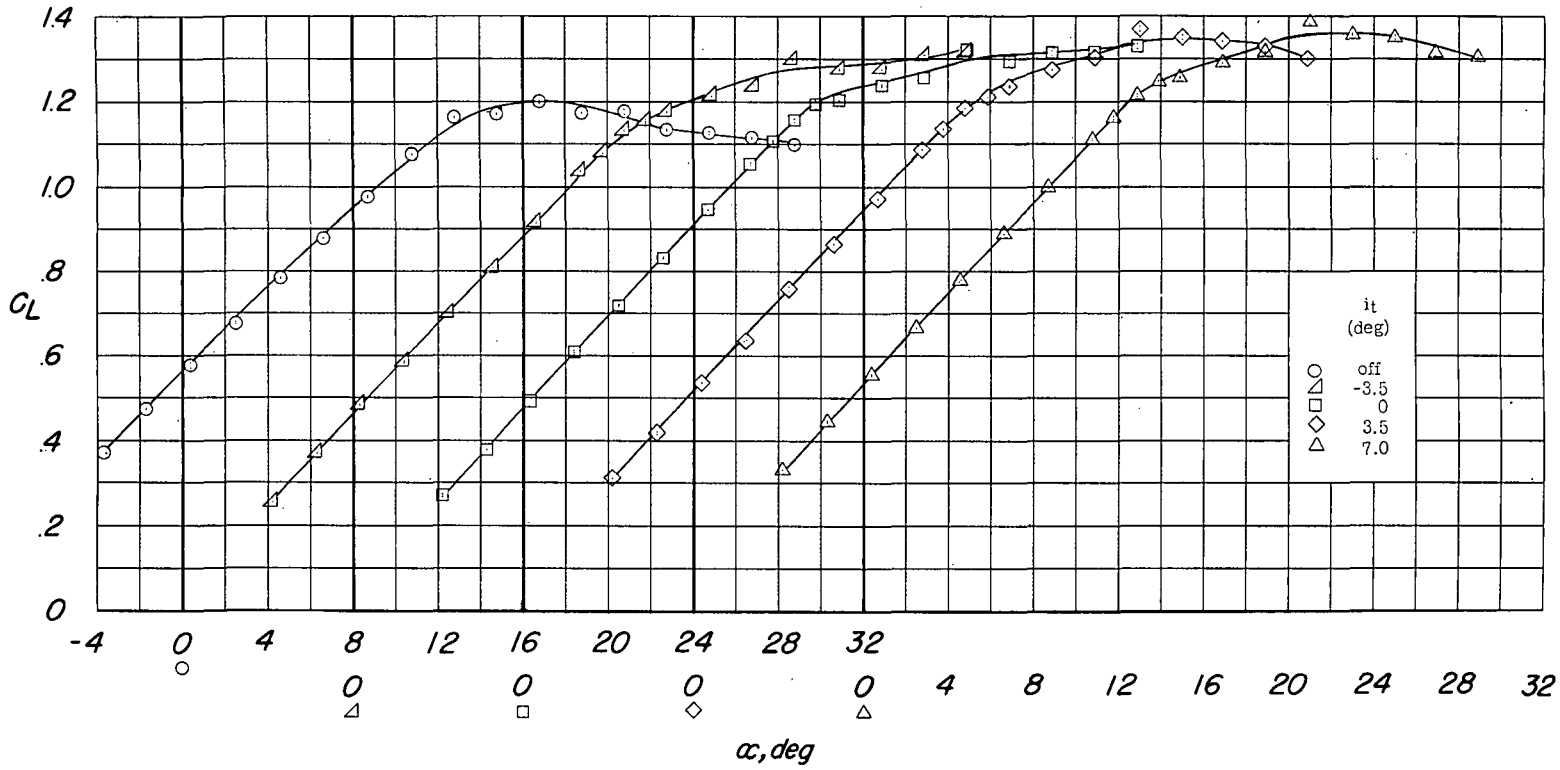

(a) C_L against α.

Figure 9.- Longitudinal stability and control characteristics of the model with the leading-edge and trailing-edge flaps deflected. Configuration A + V + $I_{SE'}$ + N_{20} + $0.7F_{46}$ + (-0.123)T.

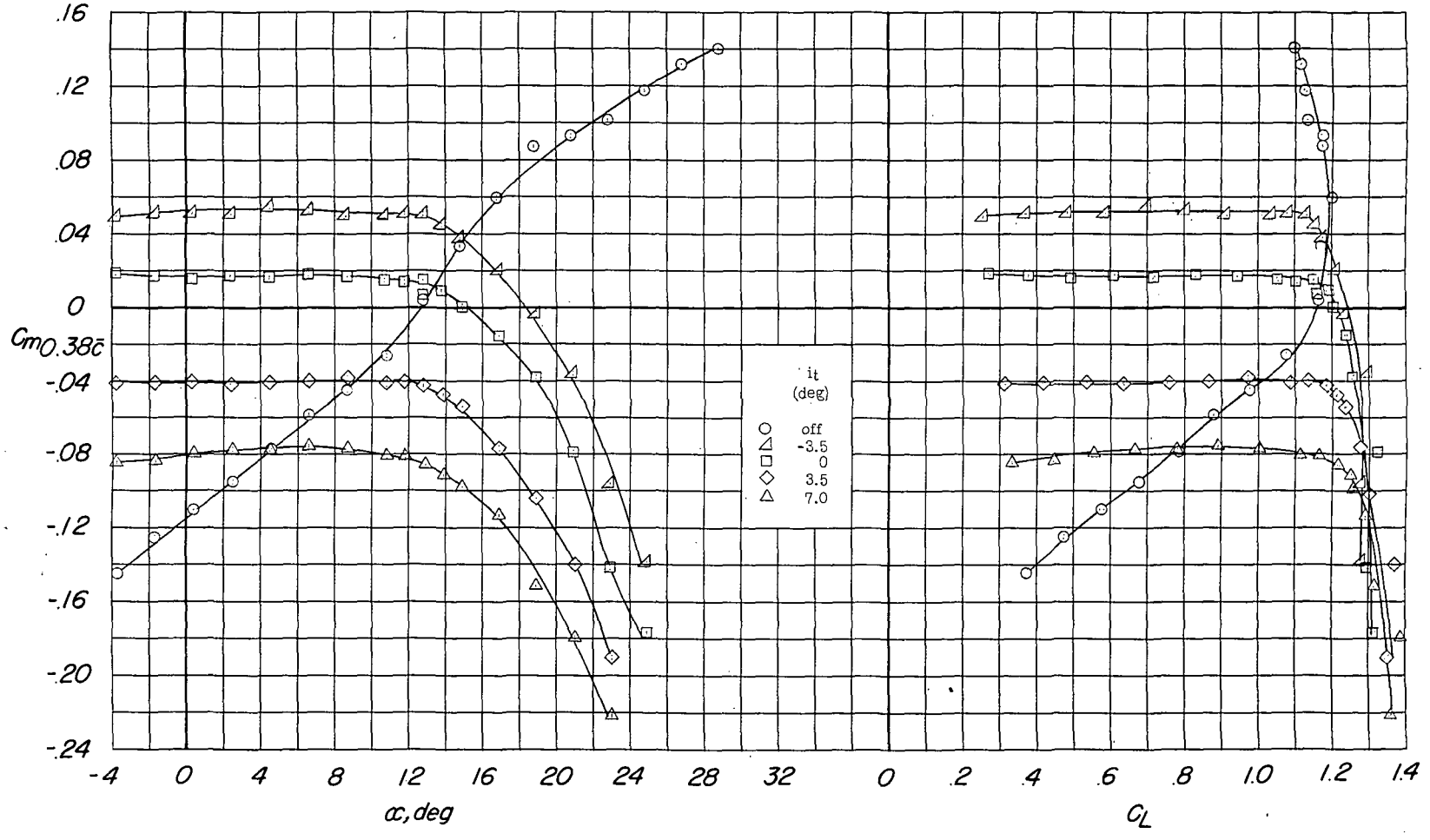

(b) $C_{m_{0.38\bar{c}}}$ against α.

(c) $C_{m_{0.38\bar{c}}}$ against C_L.

Figure 9.- Continued.

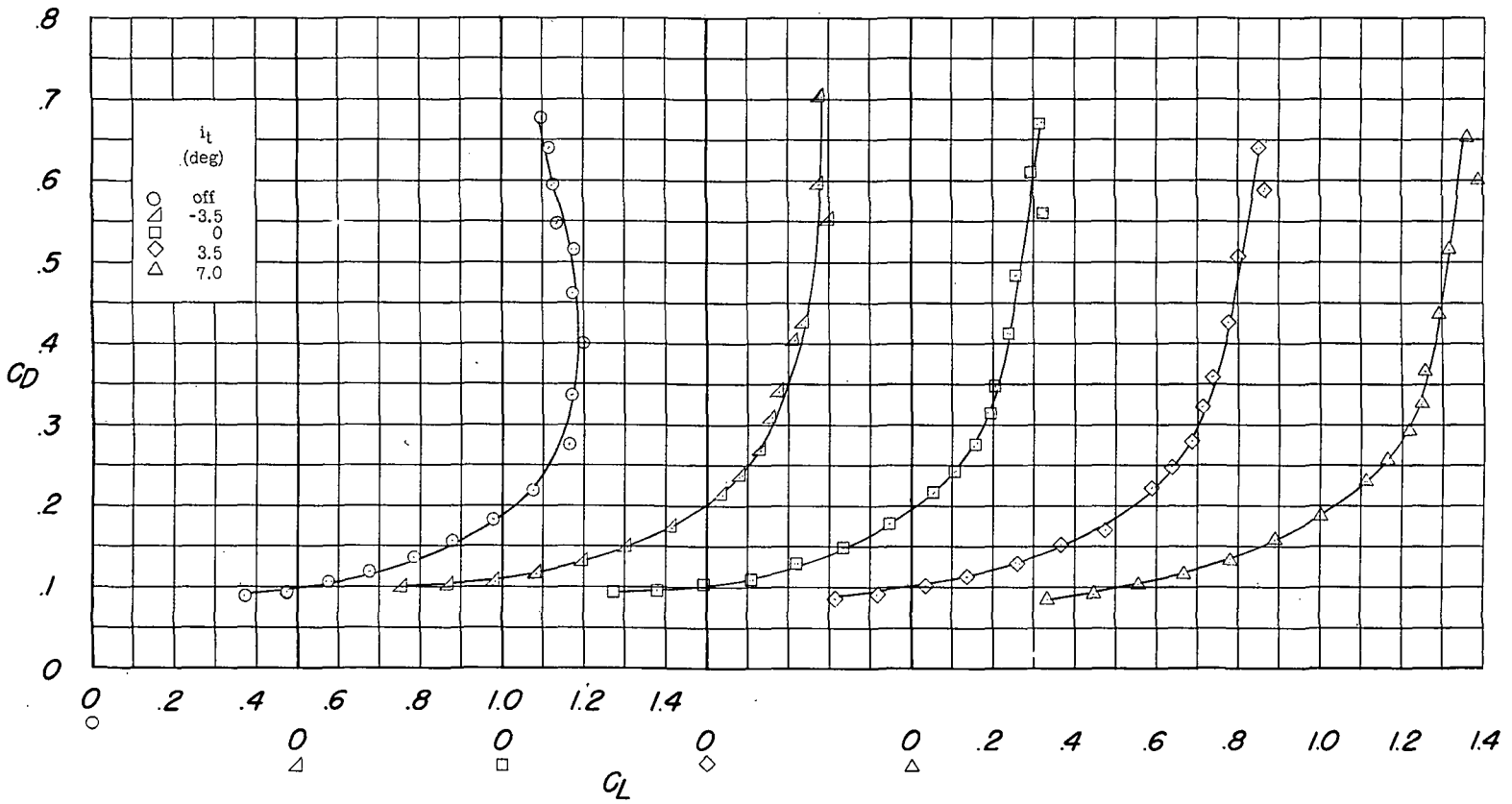

(d) C_D against C_L.

Figure 9.- Concluded.

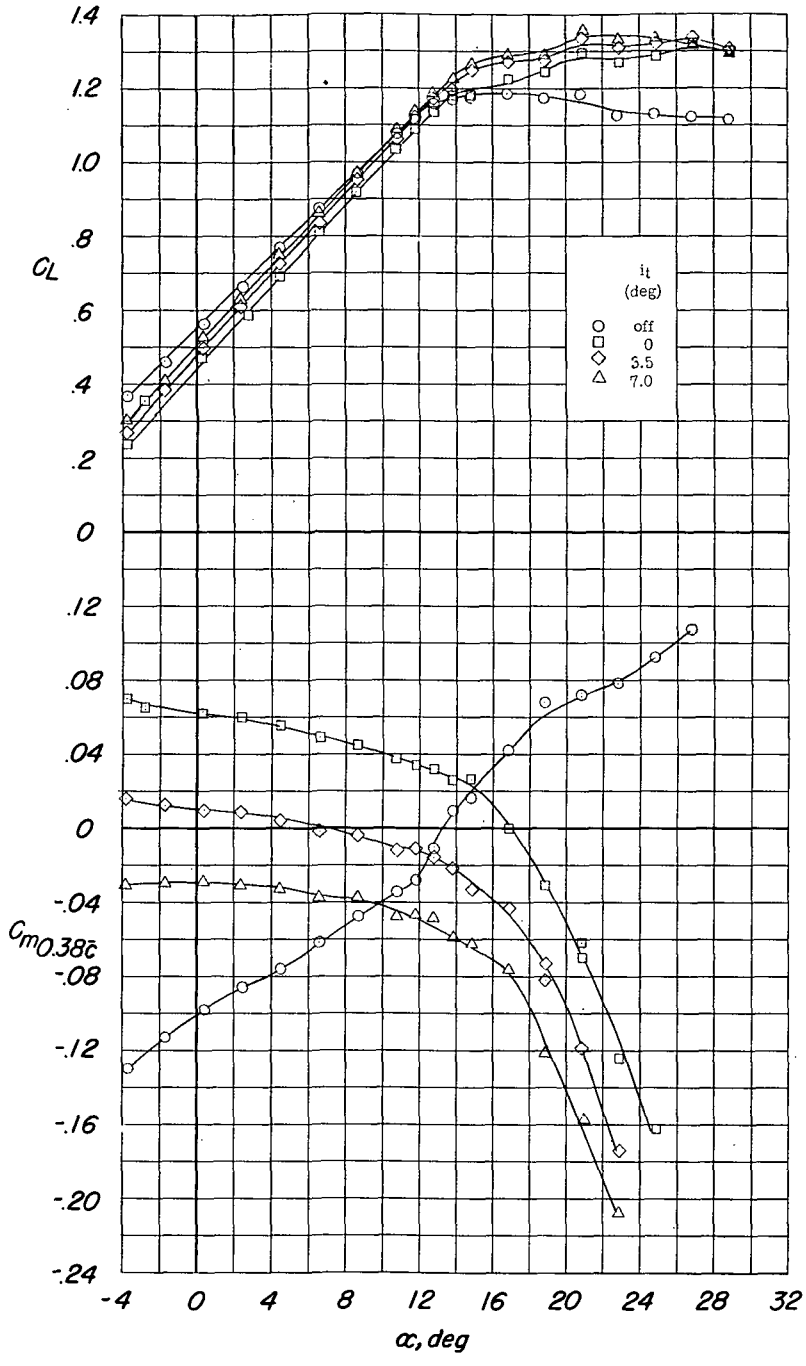

(a) C_L and $C_{m_{0.38\bar{c}}}$ against α.

Figure 10.- Longitudinal stability characteristics of the model with side speed brakes extended and with leading-edge and trailing-edge flaps deflected. Configuration A + V + $I_{SE'}$ + N_{20} + 0.7F_{46} + $B_{0,50}$ + (-0.123)T.

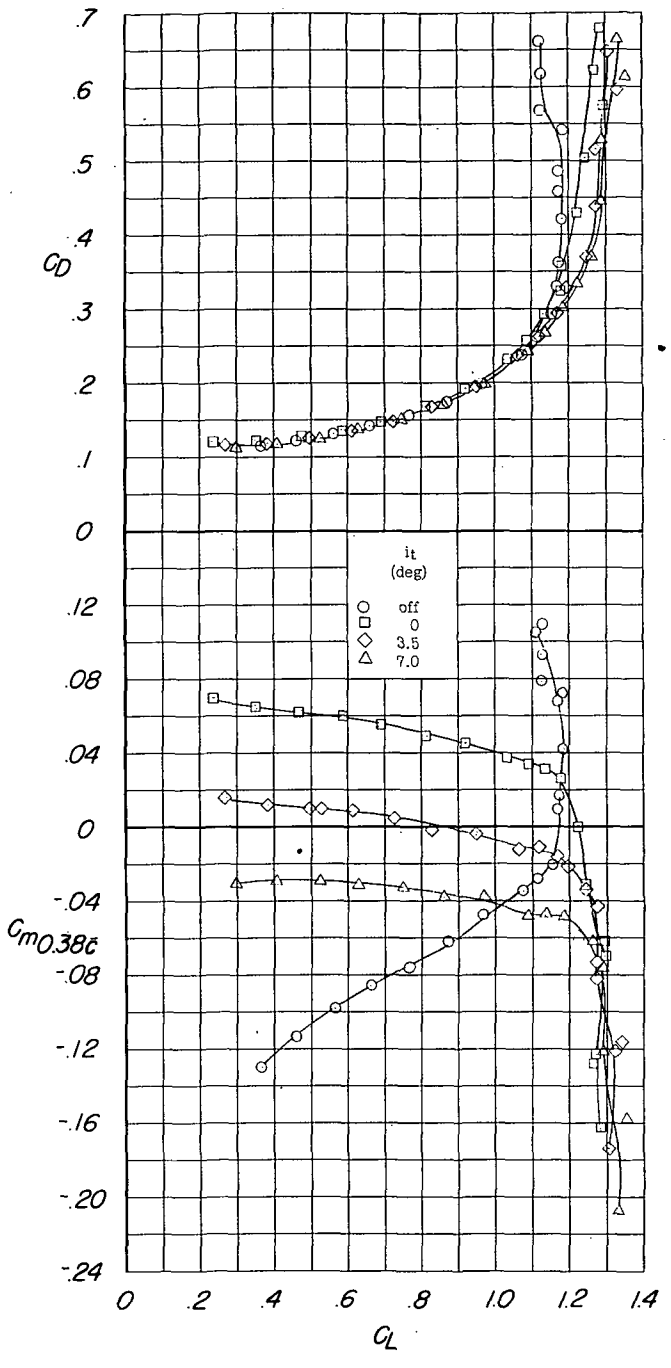

(b) C_D and $C_{m_{0.38\bar{c}}}$ against C_L.

Figure 10.- Concluded.

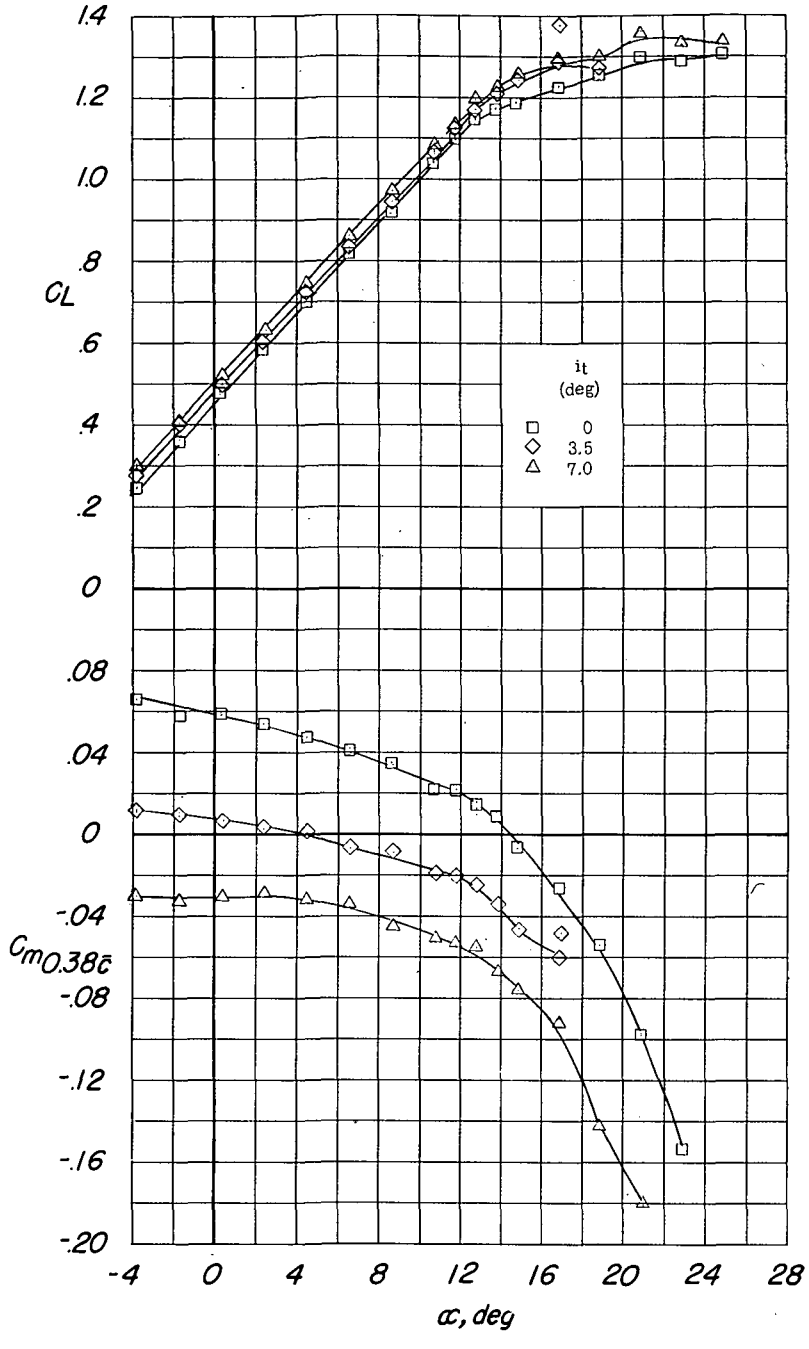

(a) C_L and $C_{m_{0.38\bar{c}}}$ against α.

Figure 11.- Longitudinal stability characteristics of the model with speed brakes extended and with leading-edge and trailing-edge flaps deflected. Configuration A + V + $I_{SE'}$ + N_{20} + $0.7F_{46}$ + $B_{50,50}$ + $(-0.123)T$.

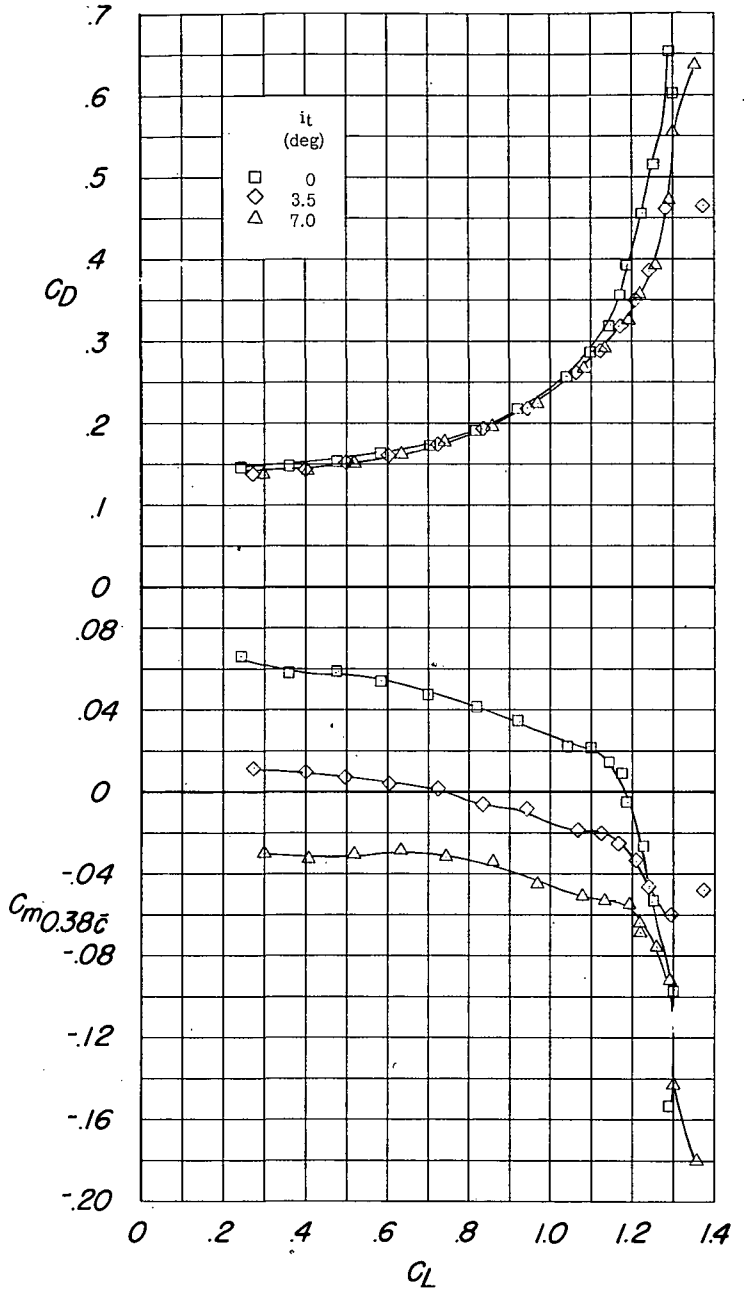

(b) C_D and, $C_{m_{0.38\bar{c}}}$ against C_L.

Figure 11.- Concluded.

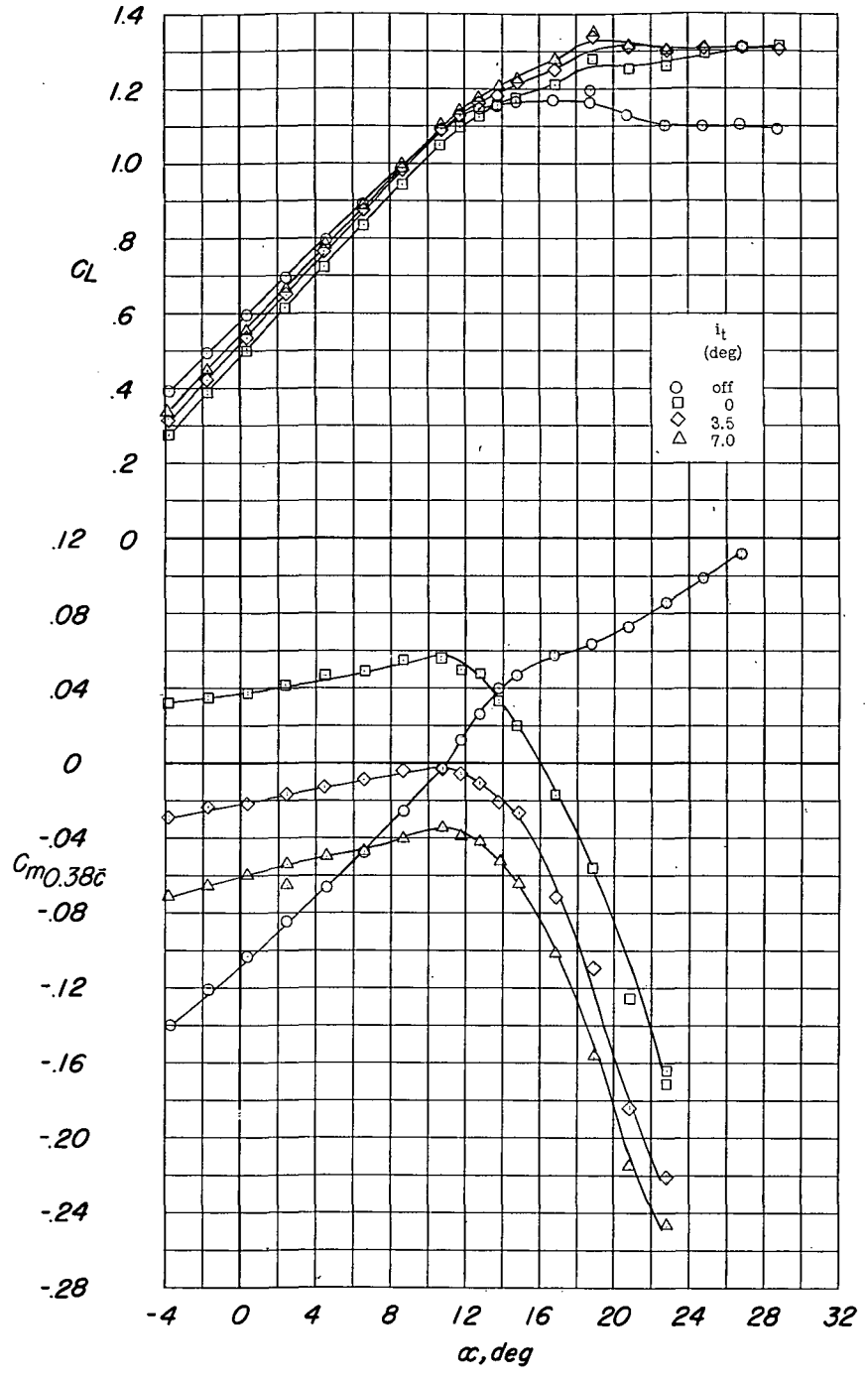

(a) C_L and $C_{m_{0.38\bar{c}}}$ against α.

Figure 12.- Longitudinal stability characteristics of the model with external stores and with leading-edge and trailing-edge flaps deflected. Configuration A + V + $I_{SE'}$ + N_{20} + 0.7F_{46} + $E_0$450 (type II) + (-0.123)T.

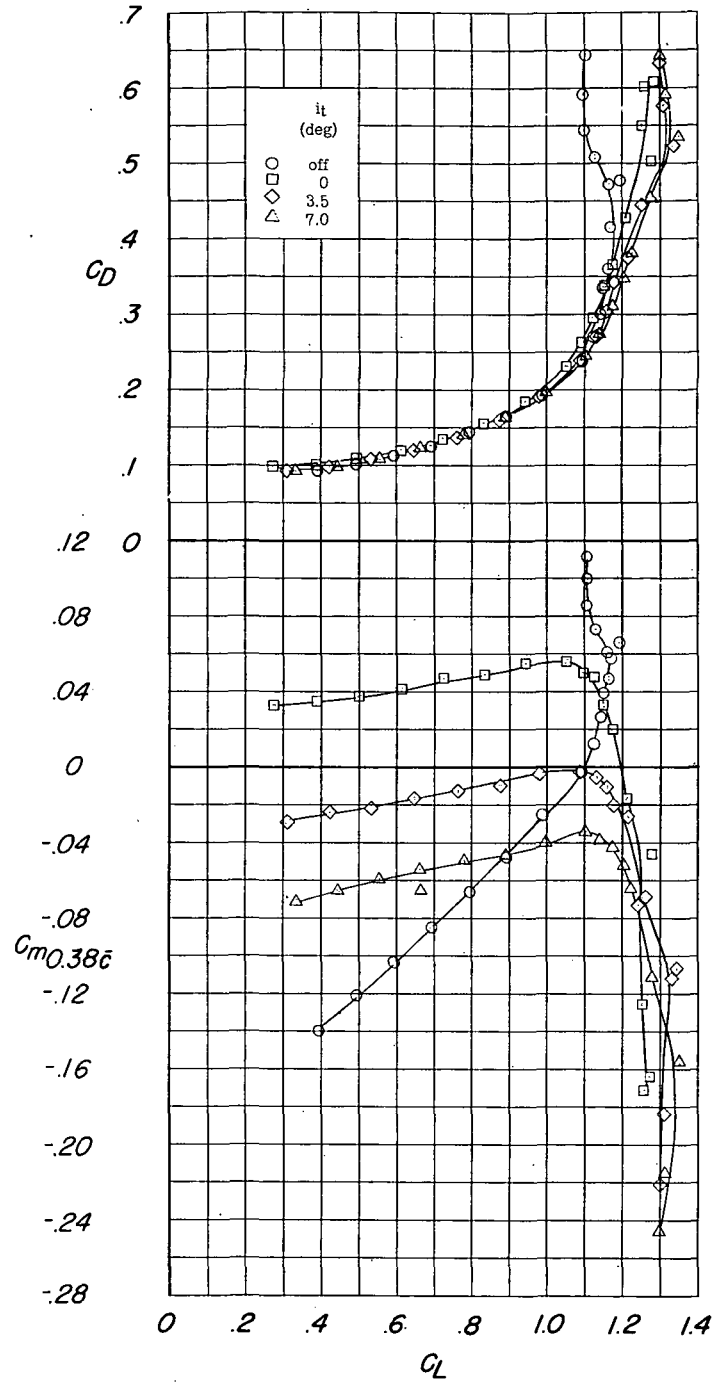

(b) C_D and $C_{m_{0.38\bar{c}}}$ against C_L.

Figure 12.- Concluded.

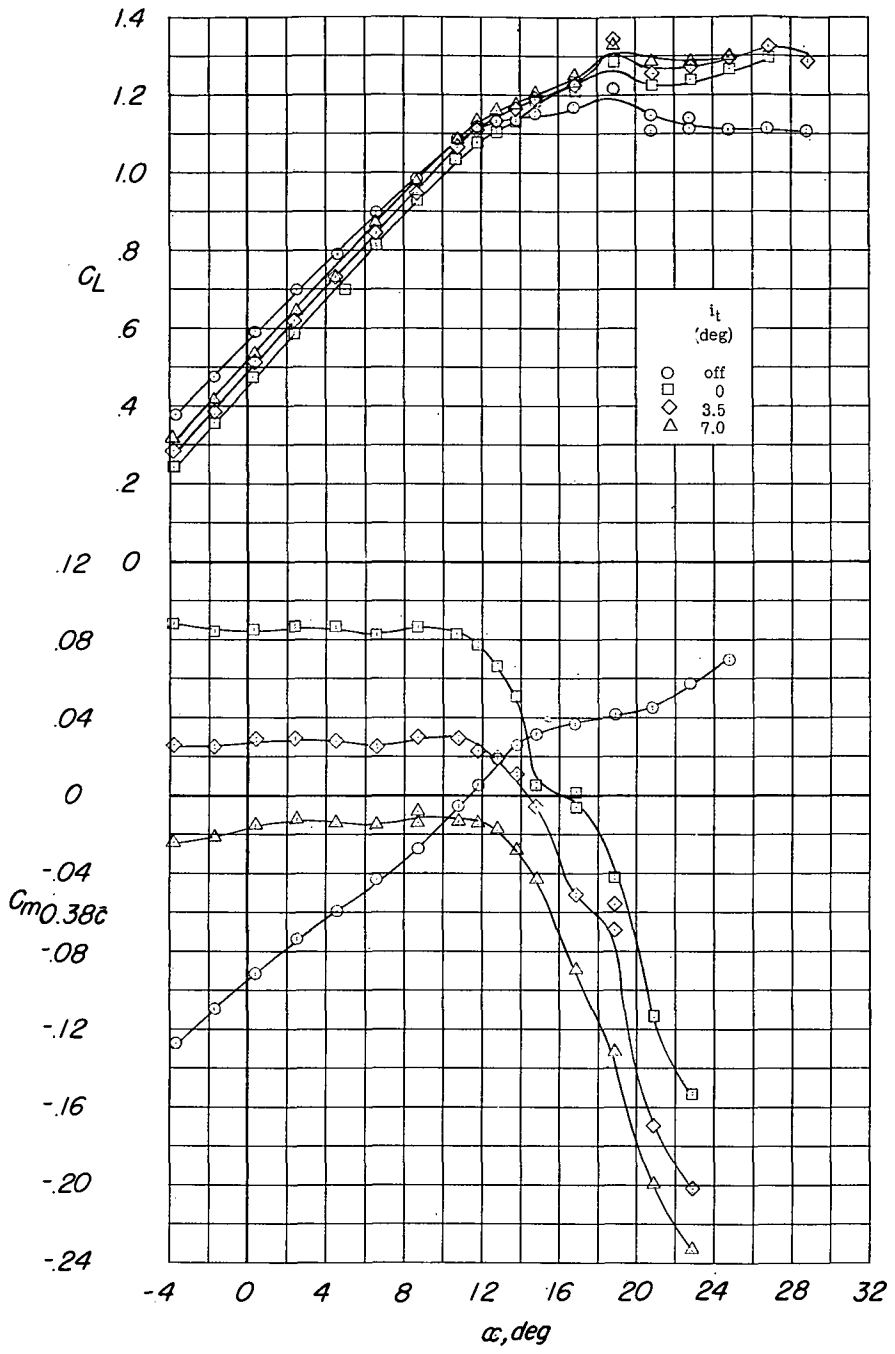

(a) C_L and $C_{m_{0.38\bar{c}}}$ against α.

Figure 13.- Longitudinal stability characteristics of the model with external stores, leading-edge and trailing-edge flaps deflected, and side speed brakes extended. Configuration A + V + $I_{SE'}$ + N_{20} + $0.7F_{46}$ + $E_0{}^{450}$ (type II) + $B_{0,50}$ + (-0.123)T.

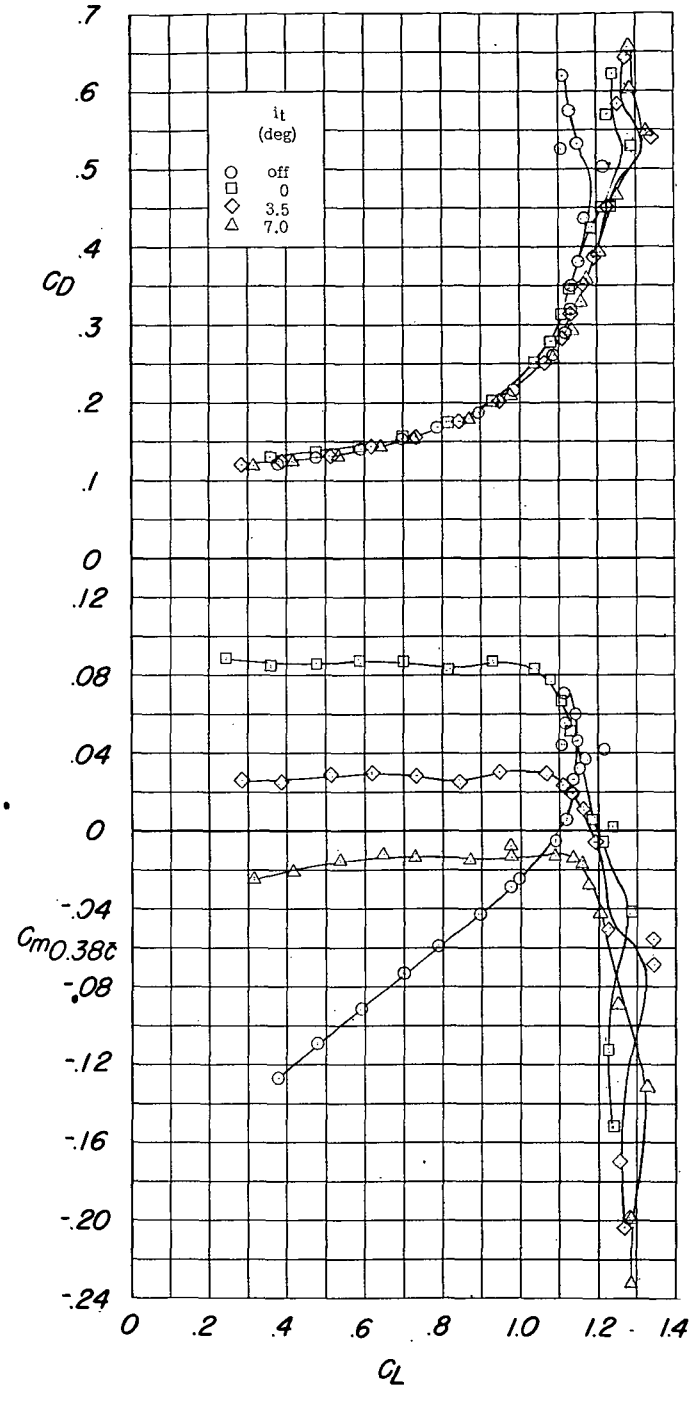

(b) C_D and $C_{m_{0.38\bar{c}}}$ against C_L.

Figure 13.- Concluded.

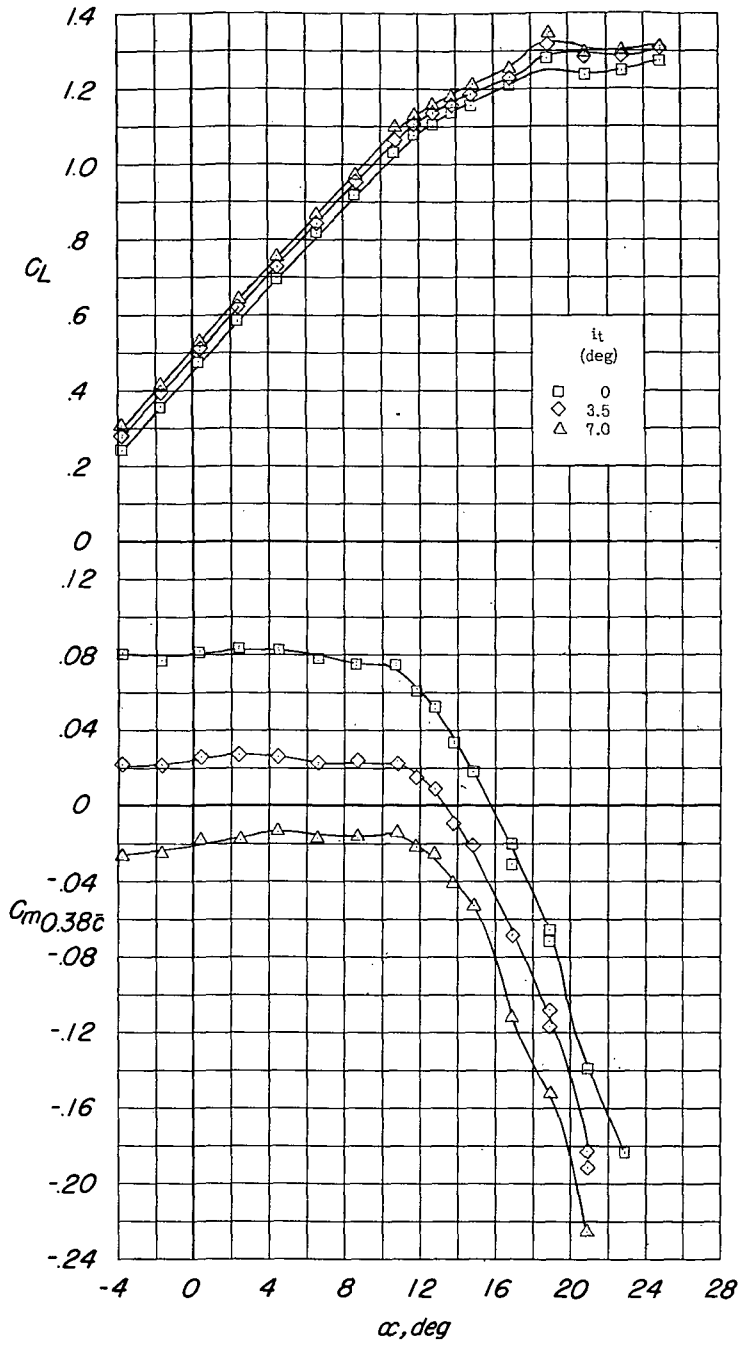

(a) C_L and $C_{m_{0.38\bar{c}}}$ against α.

Figure 14.- Longitudinal stability characteristics of the model with external stores, leading-edge and trailing-edge flaps deflected, and speed brakes extended. Configuration A + V + I_{SE}, + N_{20} + $0.7F_{46}$ + E_0450 (type II) + $B_{50,50}$ + (-0.123)T.

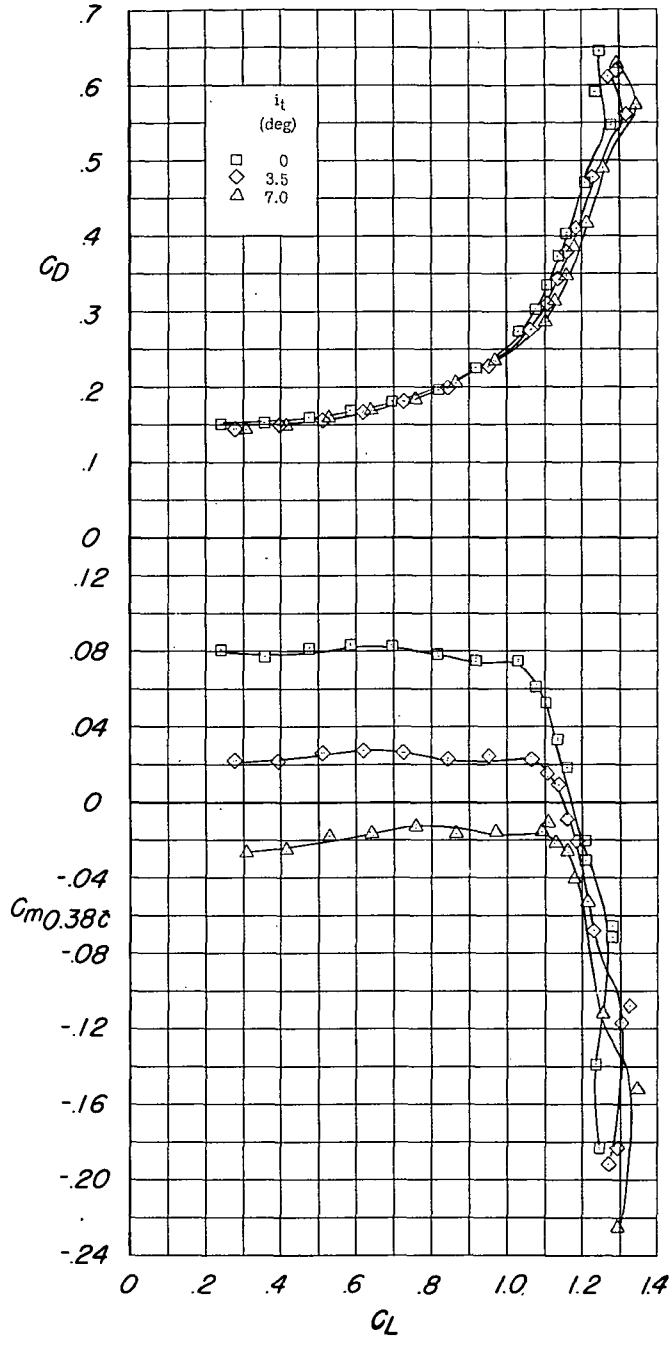

(b) C_D and $C_{m_{0.38\bar{c}}}$ against C_L.

Figure 14.- Concluded.

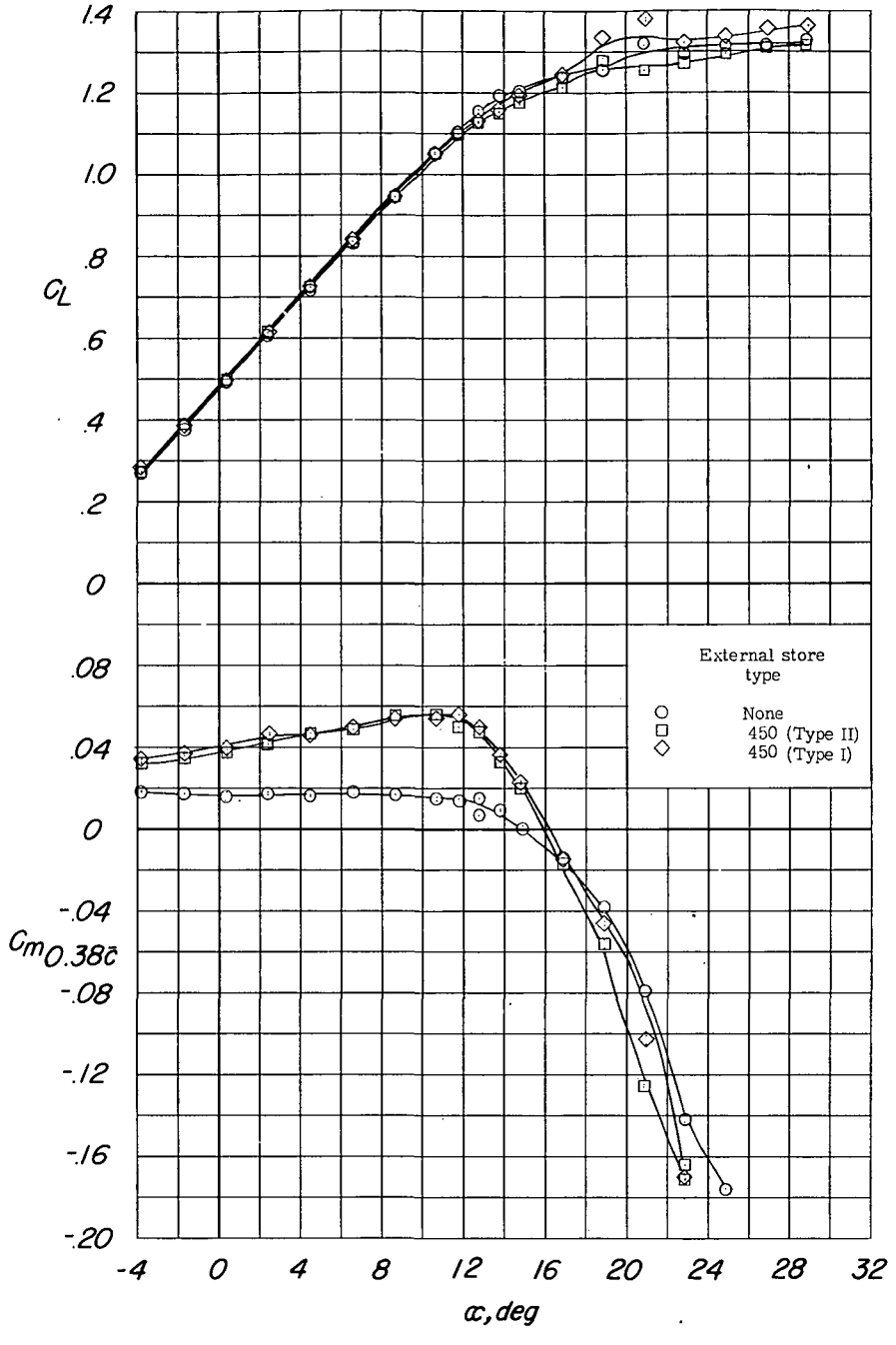

(a) C_L and $C_{m_{0.38\bar{c}}}$ against α.

Figure 15.- Longitudinal stability characteristics of the model with and without various types of external stores and with leading-edge and trailing-edge flaps deflected. Configuration A + V + $I_{SE'}$ + N_{20} + $0.7F_{46}$ + $(-0.123)T_O$ + E_O450.

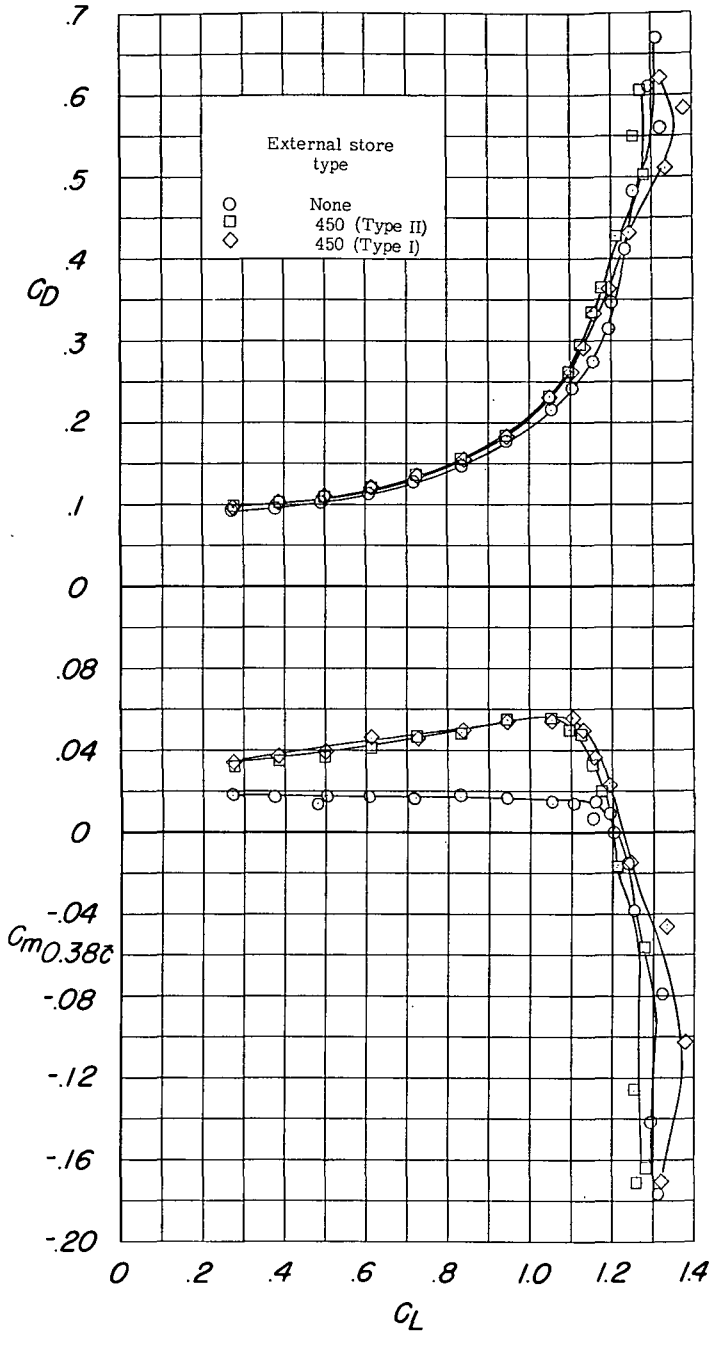

(b) C_D and $C_{m_{0.38\bar{c}}}$ against C_L.

Figure 15.- Concluded.

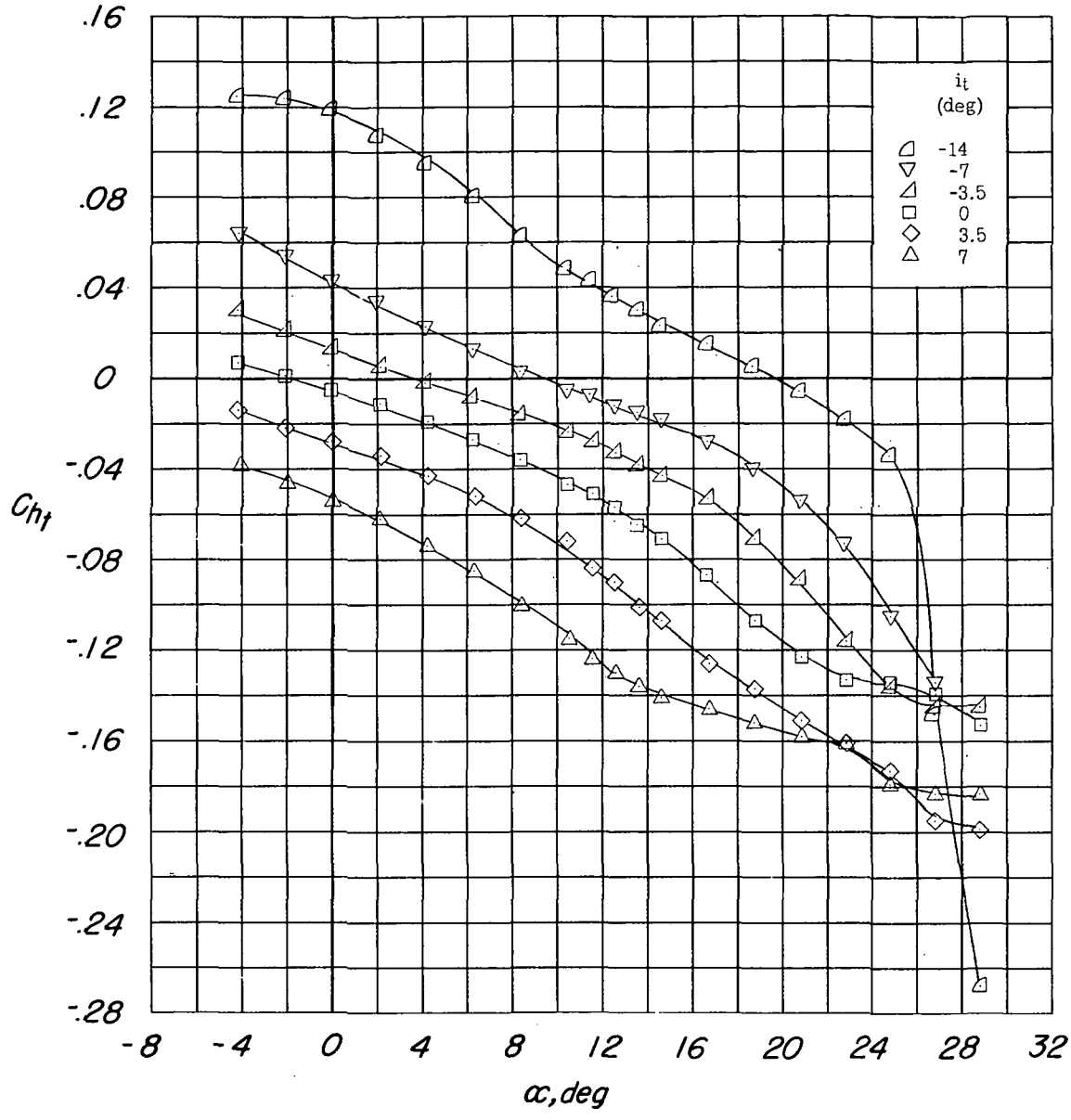

(a) C_{h_t} against α.

Figure 16.- Effects of various tail incidence settings on the tail hinge-moment coefficient C_{h_t} and the normal-force coefficient C_{N_t}. Configuration A + V + $I_{SE'}$ + (-0.123)T.

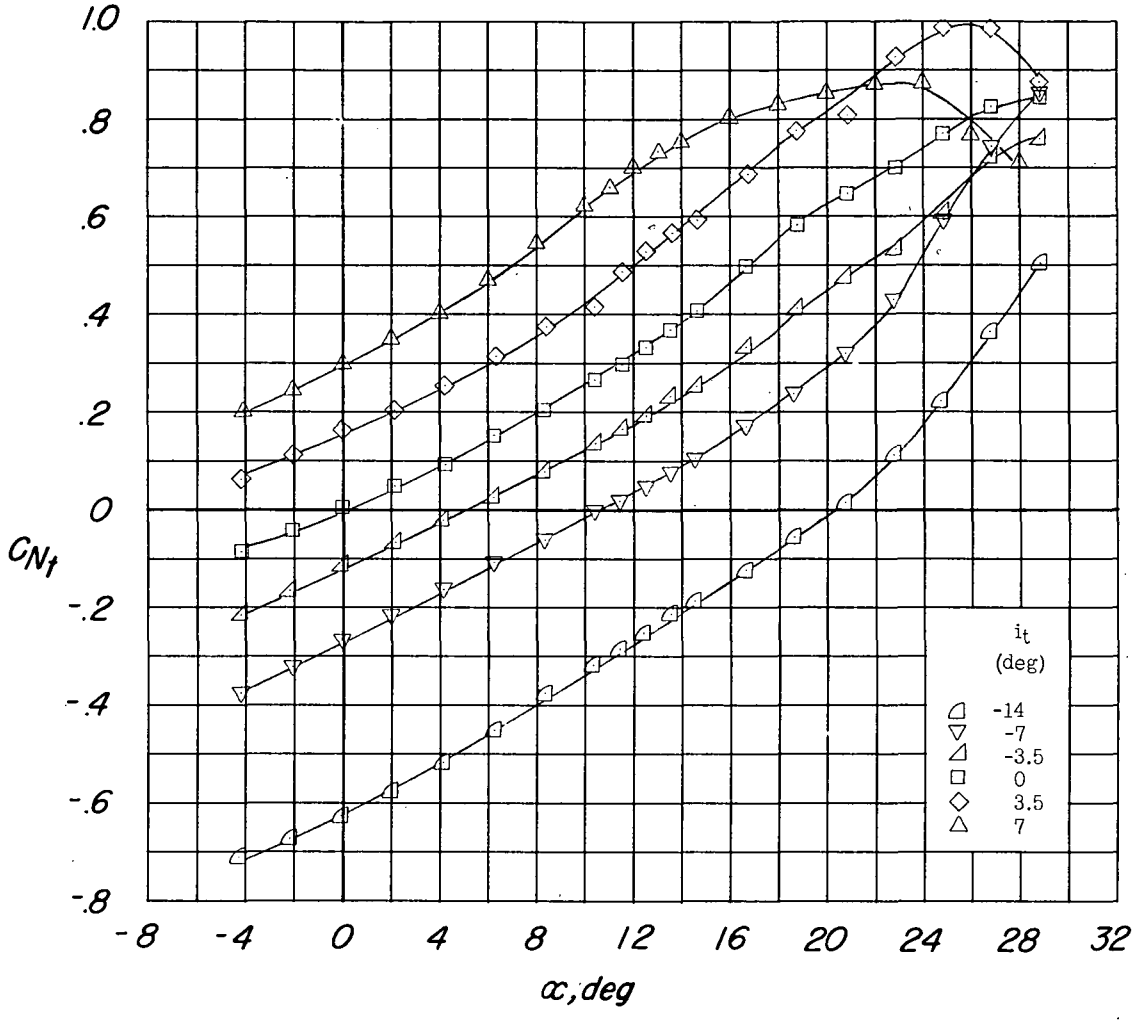

(b) C_{N_t} against α.

Figure 16.- Concluded.

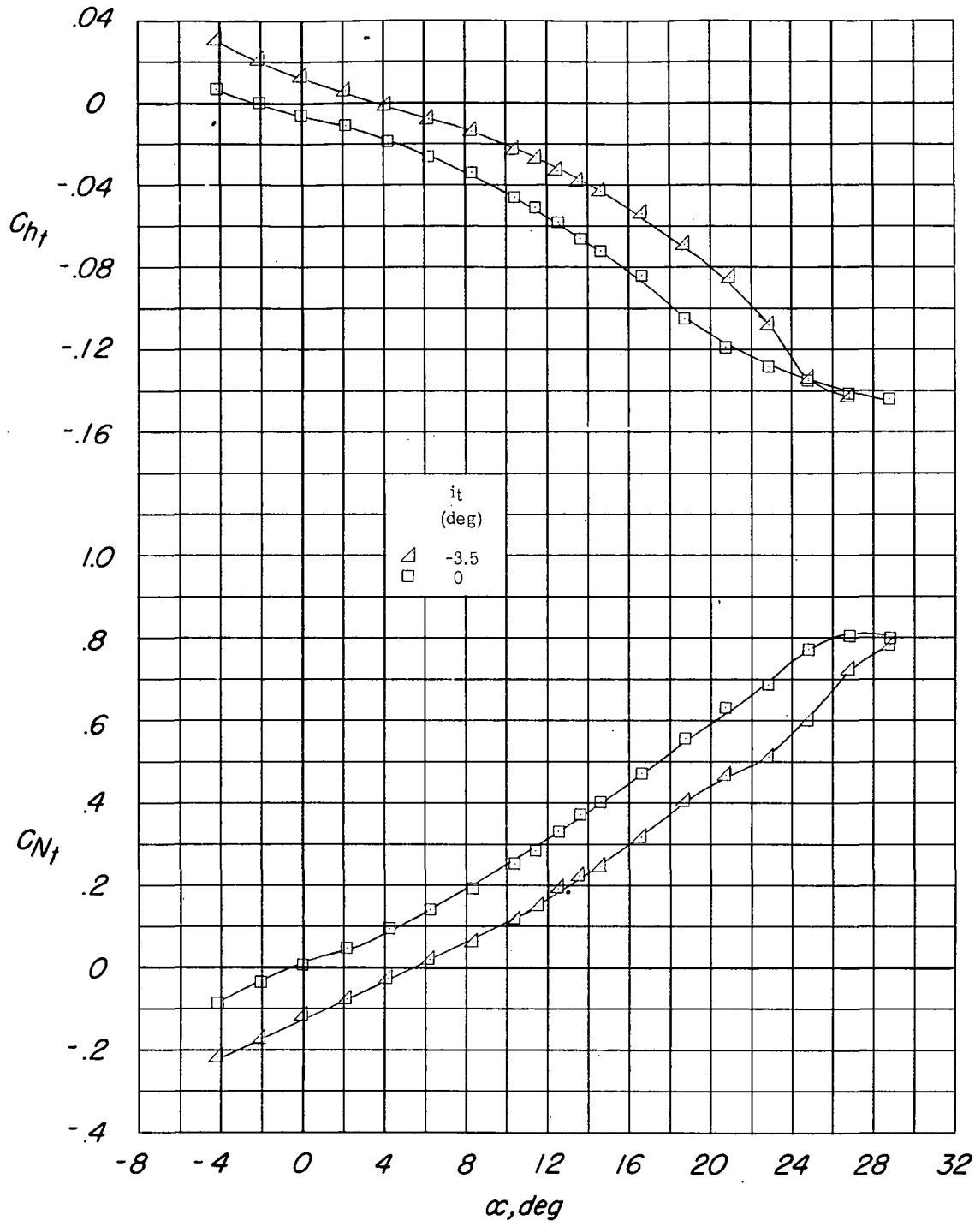

Figure 17.- Effects of various tail incidence settings on the tail hinge-moment coefficient C_{h_t} and the normal-force coefficient C_{N_t} with the drooped leading edge deflected 7.5°. Configuration A + V + $I_{SE'}$ + $N_{7.5}$ + (-0.123)T.